

AD-A215 560

78 FEB 1989



DTIC
 ELECTE
 DEC 14 1989
 S B D

MODELING THE RESPONSE OF A
 MONOPULSE RADAR TO IMPULSIVE
 JAMMING SIGNALS USING THE BLOCK
 ORIENTED SYSTEM SIMULATOR (BOSS)

THESIS

Jeffrey Keith Long
 Captain, USAF

AFIT/GE/ENG/89D-26

DEPARTMENT OF THE AIR FORCE
 AIR UNIVERSITY
AIR FORCE INSTITUTE OF TECHNOLOGY

Wright-Patterson Air Force Base, Ohio

DISTRIBUTION STATEMENT A
 Approved for public release;
 Distribution Unlimited

89 12 14 038

AFIT/GE/ENG/89D-26

MODELING THE RESPONSE OF A
MONOPULSE RADAR TO IMPULSIVE
JAMMING SIGNALS USING THE BLOCK
ORIENTED SYSTEM SIMULATOR (BOSS)

THESIS

Jeffrey Keith Long
Captain, USAF

AFIT/GE/ENG/89D-26

DTIC
ELECTE
DEC 14 1989
S B D

Public Release: Distribution Unlimited

AFIT/GE/ENG/89D-26

MODELING THE RESPONSE OF A
MONOPULSE RADAR TO IMPULSIVE
JAMMING SIGNALS USING THE BLOCK
ORIENTED SYSTEM SIMULATOR (BOSS)

THESIS

Presented to the Faculty of the School of Engineering
of the Air Force Institute of Technology
Air University
In Partial Fulfillment of the
Requirements for the Degree of
Master of Science in Electrical Engineering

Jeffrey Keith Long, B.S.
Captain, USAF

December, 1989

Public Release; Distribution Unlimited

Preface

The purpose of this research was to determine the response of two different types of amplitude comparison monopulse processors to an impulsive jamming signal for different degrees of electrical imbalance in each system. Models of the processors were implemented using the Block Oriented System Simulator (BOSS) software package.

It was determined that some angular inaccuracies resulted from any degree of electrical mismatch for both types of systems modeled. The greatest inaccuracies were seen for a monopulse processor using AGC for normalization and having more than a 5% frequency imbalance between the two parallel receiver channels.

Any research effort of this scope cannot be performed in a vacuum. I want to extend my warmest appreciation to my thesis advisor Lt Col David Meer for his patience and gentle guidance. I also want to thank Capt David Reddy of the Air Force Electronic Warfare Center for sponsoring this thesis.

Finally, I want to thank my wife Anne and our three children, Kimberly, Chelsea, and Jeffrey Sean, for their patience during my studies at AFIT. Ours is a very close family, and the unpleasantness of many hours of separation required while attending AFIT was mitigated by the knowledge that they were supporting my efforts.

Jeffrey Keith Long

Accession For	
NTIS GRA&I	<input checked="" type="checkbox"/>
DTIC TAB	<input type="checkbox"/>
Unannounced	<input type="checkbox"/>
Justification	
By _____	
Distribution/	
Availability Codes	
Dist	Avail and/or Special
A-1	

Table of Contents

	Page
Preface	ii
Table of Contents	iii
List of Figures	iv
List of Tables	v
Abstract	vi
I. Introduction	1-1
1.1 Background	1-1
1.2 Problem Statement	1-2
1.3 Summary of Current Knowledge	1-2
1.3.1 Definition of Tracking Radar.	1-2
1.3.2 Early Tracking Radar Designs.	1-3
1.3.3 Modern Monopulse Radar Systems.	1-3
1.3.4 The Previous Approach to Jamming Monopulse.	1-5
1.3.5 A New Type of Jamming Approach.	1-5
1.4 Status	1-6
1.5 Scope	1-7
1.6 Limitations	1-7
1.7 Assumptions	1-7
1.8 Equipment Required and Overview of BOSS Software	1-8
1.9 Approach	1-8

	Page
II. Amplitude Comparison Monopulse Systems	2-1
2.1 Desired Monopulse Characteristics	2-1
2.2 Antenna Beams Used in Monopulse Radar	2-1
2.3 Amplitude Comparison System using Logarithmic Amplifiers	2-4
2.3.1 A Log-Amp Model.	2-6
2.3.2 Taking the Natural Log of Complex Value.	2-7
2.3.3 The Response of the Log-Amp Receiver.	2-7
2.4 Automatic Gain Control in Monopulse Radars	2-8
2.5 An AGC Based Monopulse Processor	2-9
2.5.1 An AGC Model.	2-10
2.5.2 The Response of the AGC Based Processor.	2-11
III. BOSS Implementation of System Models	3-1
3.1 Overview of Model Implementation on BOSS	3-1
3.1.1 An Example of a BOSS Simulation.	3-2
3.2 A Log-Amp Monopulse Processor Model in BOSS	3-4
3.2.1 BOSS Primitive Modules Used.	3-5
3.2.2 Modules Built from Primitive Modules.	3-6
3.2.3 The Received Signal Generator.	3-6
3.2.4 The LN-Amplifier Module.	3-11
3.2.5 The Complex-LN Module.	3-12
3.2.6 Definition of Angular Error.	3-13
3.2.7 The Log-Amp Angular Error Model.	3-14
3.2.8 Parameters Used in the Log-Amp Models.	3-15
3.3 The AGC-Based Monopulse Processor as Modeled in BOSS	3-16
3.3.1 The General AGC Loop Modeled	3-16
3.3.2 Specific AGC Design Parameters	3-17

	Page
3.3.3 The AGC Detector Implemented in BOSS.	3-21
3.3.4 The Other BOSS Modules Unique to the AGC Model.	3-22
3.3.5 AGC System Angular Error Model.	3-23
3.3.6 Parameters Used in the AGC Model.	3-24
IV. Results	4-1
4.1 General Simulation Parameters	4-1
4.1.1 A Basic Assumption.	4-1
4.1.2 Baseline Simulations.	4-1
4.2 Determination of Calibration Constant.	4-2
4.3 Simulations to Establish the Effect of the Time of the Impulsive Jamming	4-2
4.4 Basic Noise Influence Tests	4-6
4.5 Simulation Matrices	4-8
4.5.1 Simulations with Gain Imbalances.	4-9
4.5.2 Simulations with Frequency Imbalances.	4-9
4.6 Gain Imbalance Results	4-10
4.7 Frequency Imbalance Results	4-12
4.7.1 Log-Amp Frequency Imbalance Results.	4-14
4.7.2 AGC Frequency Imbalance Results.	4-15
V. Conclusions and Recommendations	5-1
5.1 Conclusions	5-1
5.1.1 Impact of Imbalanced Systems Without Impulsive Jamming.	5-1
5.1.2 Errors Introduced as a Result of an Impulsive Jamming Signal.	5-2
5.1.3 Timing of Impulse and Effect of Noise Upon Induced Errors.	5-3

	Page
5.1.4 Interpretation of the Sign of the Error.	5-3
5.2 Recommendations	5-4
Appendix A. AGC Reaction to Impulsive Signal	A-1
Bibliography	BIB-1
Vita	VITA-1

List of Figures

Figure	Page
1.1. Monopulse Antenna Patterns	1-4
2.1. The Four Squinted Beams Used in a Typical Amplitude Comparison Monopulse Radar	2-2
2.2. The Cross Section of the Four Beams used in an Amplitude Comparison Monopulse Radar	2-2
2.3. Amplitude Comparison Monopulse Patterns in either coordinate: sum(s), difference (d), squinted beams (v_1 and v_2), and the normalized difference ratio ($\frac{d}{s}$).	2-3
2.4. Block Diagram of Logarithmic Amplifier Monopulse Processor	2-5
2.5. Outputs of $\ln v_1/v_2 $ Processor and Exact Processor vs Angle	2-8
2.6. Block Diagram of Monopulse Processor Using AGC	2-9
2.7. Outputs of an Exact and an AGC-Type Processor, as a Function of Target Angle	2-12
3.1. A Simple Log-Amp Model	3-2
3.2. BOSS Implementation of the Simple Log-Amp Model	3-3
3.3. The Log-Amp System as Modeled in BOSS	3-4
3.4. The BOSS Received Signal Generator Module	3-7
3.5. An example of the Output of the Received Signal Generator module	3-9
3.6. The output of the Received Signal Generator module showing the relationship of v_1 to v_2 as the "Angle off Boresight" parameter is varied from -8 milliradians to $+8$ milliradians	3-10
3.7. BOSS Implementation of the Log-Amp	3-11
3.8. BOSS Module to take Natural Logarithm of Complex Signal	3-13
3.9. A Boss Model to Compute Induced Angular Errors	3-15

Figure	Page
3.10. The AGC-Type Monopulse Processor as Modeled in BOSS	3-17
3.11. Desired Response of IF Amplifier to AGC Voltage	3-18
3.12. The AGC Detector Module Implemented in BOSS	3-20
3.13. AGC-Type System Model for Calculation of Angular Errors	3-23
4.1. Baseline Monopulse Ratio Plot for Log-Amp System	4-3
4.2. Baseline Monopulse Ratio Plot for AGC System	4-4
4.3. Angular Errors Induced in Both Log-AMP and AGC-Type Monopulse Systems for an Impulse Applied During Received Pulse #1, #4, or #8 in a Train of 10 Pulses under Balanced Conditions	4-5
4.4. Angular Errors in a Balanced, Log-Amp System due to AWGN in Conjunction With an Impulse	4-7
4.5. Angular Errors in Log-Amp System Output for a 5% Gain Imbalance (with and without an impulse applied)	4-11
4.6. Angular Errors in an AGC-Type System for 5% Gain Imbalance (with and without an impulse applied)	4-13
4.7. Angular Errors Induced in Log-Amp System as a Function of Frequency Imbalance, <i>No Impulse Applied</i>	4-14
4.8. Angular Errors Induced in Log-Amp System as a Function of Frequency Imbalance, <i>With Impulse Applied</i>	4-15
4.9. Angular Errors Induced in AGC Based System as a Function of Frequency Imbalance, <i>No Impulse Applied</i>	4-16
4.10. Angular Errors Induced in AGC Based System as a Function of Frequency Imbalance, <i>With Impulse Applied</i>	4-17
4.11. Increase in Magnitude of Angular Errors Induced in AGC Based System as Frequency Imbalance Becomes Increasingly Positive, <i>With Impulse Applied</i>	4-18
A.1. IF Filter Output Showing Effect of AGC Gain	A-1
A.2. AGC Gain Control Voltage, Normal Operation	A-2
A.3. IF filter Output with Impulse Applied at T=2.0 seconds	A-3

Figure	Page
A.4. Control Signal Showing Impact of the Impulse for Several Pulse Periods	A 4

List of Tables

Table	Page
3.1. The Significant Parameters Used in the Log-Amp System Simulations	3-25
3.2. The Significant Parameters Used in the AGC System Simulation	3-24
4.1. Gain Imbalance Runs for Both LOG-AMP and AGC-Type System	4-9
4.2. Frequency Imbalance Simulations for AGC-Type System	4-9
4.3. Frequency Imbalance Simulations for LOG-AMP Type System	4-10

Abstract

The purpose of this study was to develop computer models of two types of amplitude comparison monopulse processors using the Block Oriented System Simulation (BOSS) software package and to determine the response to these models to impulsive input signals. This study was sponsored by the Air Force Electronic Warfare Center at Kelly AFB in an effort to determine the susceptibility of monopulse tracking radars to impulsing jamming signals.

Two types of amplitude comparison monopulse receivers were modeled, one using logarithmic amplifiers and the other using automatic gain control for signal normalization. Simulations of both types of systems were run under various conditions of gain or frequency imbalance between the two receiver channels. The resulting errors from the imbalanced simulations were compared to the outputs of similar baseline simulations which had no electrical imbalances.

The results of the analyses showed that the accuracy of both types of processors was directly affected by gain or frequency imbalances in their receiver channels. In most cases, it was possible to generate both positive and negative angular errors, dependent upon the type and degree of mismatch between the channels. The system most susceptible to induced errors was a frequency imbalanced processor which used AGC circuitry. This research also demonstrated that any errors introduced will be a function of the degree of mismatch between the channels and therefore would be difficult to exploit reliably. It is recommended that further research be conducted with both amplitude and phase comparison monopulse processors to further quantify the nature of the errors that can be introduced into these systems with an impulsive jamming signal.

MODELING THE RESPONSE OF A MONOPULSE
RADAR TO IMPULSIVE JAMMING SIGNALS
USING THE BLOCK ORIENTED SYSTEM SIMULATOR (BOSS)

I. Introduction

1.1 Background

A critical factor in the survivability of a modern aircraft in today's complex electronic combat arena is the ability to avoid detection by the front-line search and tracking radars used by most countries to protect their borders. In addition to detection of incoming aircraft, search and tracking radars are also used extensively in the target acquisition and terminal guidance of many ground-to-air and air-to-air missiles.

The traditional approaches to countering the threat of tracking radars has been centered on jamming them with emissions of high-power energy or on attempts to "fool" the radar or its operator with signals that resemble the anticipated echo but which convey incorrect information concerning the target's location or actions. Although these can be effective countermeasures, they do have their price. In order to capture the circuitry in the radar receiver, the jamming signal had to contain more energy than the echo from the target. The higher energy jamming signal may call more attention to the intruding aircraft than the aircraft's presence alone might warrant.

Research has begun on a different jamming tactic, one that researchers hope will degrade the performance of a tracking radar without transmitting the easily detected, high energy signal. The theory is that, by transmitting a pulse of energy

with a very narrow time-duration, the new jamming method can cause considerable degradation in a tracking radar without drawing undue attention to the jammer itself. My thesis effort will address a method of predicting the effectiveness of such a jammer on a typical tracking radar system.

1.2 *Problem Statement*

This thesis will develop a model of a monopulse radar receiver using a computer simulation tool known as the Block Oriented System Simulator (BOSS). This model will be used to assess the impact of impulsive jamming given various degrees of frequency and gain imbalances within the receiver model.

A prerequisite to extensive research and development of this new jammer is the ability to predict the jammer's effectiveness against a typical tracking radar. Software simulation of an intended victim radar would provide a means of evaluating the proposed jamming technique's effectiveness. The development of a complete computer simulation of a radar system can involve extensive programming effort, and exploring different system configurations would require a different program for each configuration. BOSS is intended to ease the generation of computer simulations of communication systems. If accurate models of monopulse radar systems can be implemented using this computing tool, the effectiveness of a proposed jamming technique could be predicted, and the impact of electrical imbalances in the victim radar system when acted upon by the proposed jamming signal could be explored.

1.3 *Summary of Current Knowledge*

1.3.1 Definition of Tracking Radar. Skolnik defines a tracking radar system as one which measures the coordinates of a target and provides the data which can be used to predict the future location of a target. As he points out, almost any radar could function as a tracking radar if its outputs were processed correctly, but "... it is the method by which *angle tracking* is accomplished which distinguishes what is

normally considered a tracking radar from any other radar." [12:152].

1.3.2 Early Tracking Radar Designs. The earliest tracking radars were the "sequential lobing" systems in which a single pencil beam was switched from one side of the centerline of the tracking axis to the other side, with the difference in amplitudes of the received signals indicating the angular displacement of the target. To measure angular displacement along an orthogonal axis, two other beam positions are required. The primary limitations of these tracking radars were the fact that the overall accuracy was limited by the need for equality of the receiving channel as each of the beam positions was selected, and the need for multiple pulses of energy before the measurement can be completed.

The next design was an extension of the sequential lobing radar known as a "conical scanning" radar. In this system, instead of stepping the radar beam around the target's position in discrete increments, the antenna beam was rotated about a cone centered along the boresight of the tracking axis. To obtain information about the target's position along a pair of orthogonal axes, it was necessary to transmit and receive at least four times during one revolution of the antenna beam. The need for a discrete number of pulses to determine the target's position once again invited errors which would limit the accuracy of the measurement. If the target's return echo changed appreciably from one pulse to the next during a single scan (as might be caused by target glint or changing orientation), this difference in received amplitude would induce errors in the measurement of the target's angular position [9:4].

1.3.3 Modern Monopulse Radar Systems. Unlike the two systems mentioned above, a monopulse radar system is able to gather all of the information it requires from a single transmitted pulse (hence 'mono'-pulse) of energy. Special receive antenna patterns are used to determine the target's position along two orthogonal axes. One usually talks of the azimuth plane, corresponding to directions along the horizon and the zenith plane, corresponding to movement at right angles to the azimuth

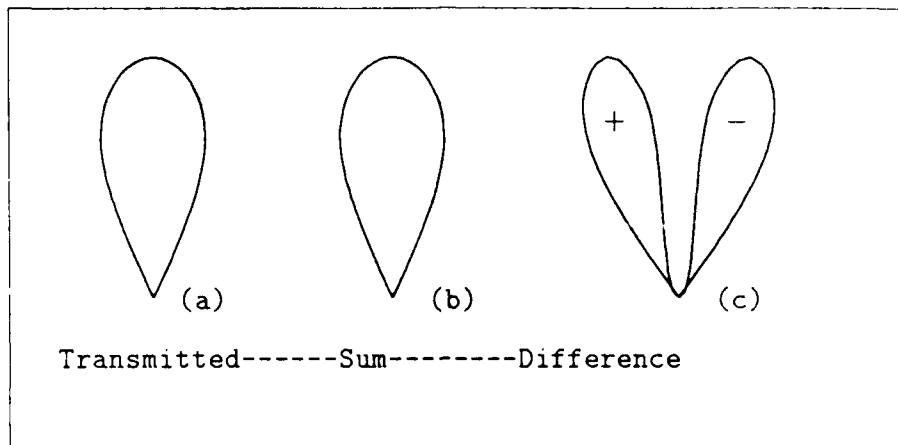


Figure 1.1. Monopulse Antenna Patterns

plane [12:160]. Following the transmission of a single pulse of RF energy using the transmit beam (see Figure 1.1 (a)), the energy returning from the target is detected simultaneously in the sum antenna pattern and the difference antenna pattern (see Figure 1.1 (b) and (c)). The signals from the two antenna patterns are processed in two nearly identical receiver channels. Since no two physical or electronic elements can be made exactly identically, there will be some inevitable degree of mismatch of the electrical characteristics of the two receiver channels. As we will see later, this electrical mismatch could be exploited by an Electronic Countermeasures (ECM) signal. The ratio of the difference pattern to the sum pattern is used to determine the direction to the target. If the radar's antenna is pointing directly at the target, this ratio will establish a signal level consistent with a correct detection of the target's angular position. If this signal ratio can be intentionally disturbed without the radar system detecting the interference, then the radar could be made to indicate an incorrect target position.

1.3.4 The Previous Approach to Jamming Monopulse. In the past, one of the more common ECM techniques used against monopulse radars was to employ a

'noise' jammer directed at the receiving antenna of the monopulse radar. The noise jammer transmitted a high power, broad-band RF energy signal which was spread across the band of frequencies that the threat radar (in this case, the monopulse tracker) uses for its operation. By flooding the radar's receiver with extraneous return signals, the jamming aircraft hoped to deny the radar the opportunity to detect it by lowering the sensitivity of the receiver circuitry as the receiver adjusted its gain to try to copy with all of the extraneous signals it was receiving. This method of jamming a monopulse radar worked quite effectively if enough power was transmitted. More sophisticated means of confusing or interfering with the proper interpretation of the return signal from a target have also been devised, but once again, all of these methods depend upon drawing the radar's attention away from the actual target by means of a signal which must have at least as much energy as the target's actual echo signal contains. Unfortunately, the act of jamming can draw more attention to the jammer than most crews would like, especially since today's "smart" missiles are capable of detecting when they are being jammed and then switching into a 'home-on-jam' mode of guidance in which the jamming signal acts as a beacon, aiding the missile in locating its intended target.

1.3.5 A New Type of Jamming Approach. In the past year or two, a company called Power Spectra Incorporated (PSI) of San Francisco, CA, has developed a device which will, for the first time, be able to generate bursts of RF energy which occur quickly enough to be classified as 'impulses.' The basic idea of an impulsive jamming signal is that, while there is a great deal of power in the pulse itself, it occurs so quickly that there is very little energy to give away the jammer's location. According to Mr. Steve Davis of PSI [3], their new devices are capable of generating pulses with durations of less than 100 pico-seconds.

Since devices of this type have not existed until recently, no one except Capt Dennis Tackett has explored the effects of an impulsive signal once it has been received by a monopulse radar. In his research, Capt Tackett explored the response

of the type of filter used in most monopulse radars when they were excited by a true impulse signal [13].

A true impulse, as defined by mathematicians and used by engineers for theoretical work, is not realizable. This theoretical impulse has infinite height (power) and exists for a discrete time interval of infinitely narrow duration.

From linear system theory, we know that when an impulse is input to a filter (such as those found in a radar receiver's IF section), the filter's output will rise quickly and then decay back through zero and exhibit a dampened oscillation about zero for a considerable period of time after the impulse has disappeared from the input. The rise time and duration of the oscillation converging to zero are a factor of the specific circuit component values for an individual filter. Given the fact that there will be some inevitable degree of component mismatch between the sum and difference channels of the monopulse receiver, these two channels will exhibit slightly different impulse response curves. This difference in the impulse responses of the sum and difference channels could lead to tracking errors in the presence of impulsive jamming signals.

1.4 Status

To date, the response of a monopulse radar to an impulsive signal has not been documented in the literature. This is probably due to the fact that until a few years ago, nearly ideal impulse signals (those having sufficiently narrow pulse widths) were impossible to generate. Now that the generation of such signals is possible, it is important that the reaction of various components of a monopulse radar to these signals be examined.

1.5 Scope

In order to make the monopulse radar model manageable, this thesis will be limited to the most common (and simplest) monopulse radar configurations, the

amplitude comparison systems. Two systems will be developed, one which will use logarithmic amplifiers in the receiver channels, and another which will use an Automatic Gain Control (AGC) circuit to provide the necessary dynamic range. The input signals will be generated from a model of the received antenna patterns as a single target moves from a position just off one side of the antenna boresight to an equal distance on the other side of the boresight.

1.6 Limitations

Amplitude comparison systems are non-coherent and the effect of phase differences between the response of the two receiver channels will not be considered. To further limit the complexity of the model, those components which are known to have *nearly* ideal impulse responses (an ideal response would pass the impulse unaffected) will not be included. Although a complete monopulse radar must include at least two identical processors, one for the azimuth plane and one for the elevation plane, the processor for only one plane will be modeled.

1.7 Assumptions

The following assumptions were made in the development of the radar model:

1. The antenna couples the impulsive input signal ideally to its output.
2. All waveguide and plumbing hardware exhibit ideal impulse response.
3. The microwave mixer is assumed to have ideal coupling characteristics.

The *first assumption* is based upon the fact that the bandwidth of the antenna must by design be wide enough to allow the frequencies used by the radar to pass through with minimal amplitude degradation. Since the impulsive signal will contain a broad spectrum of frequencies covering this entire passband, the impulsive signal at the pertinent frequencies will pass through the antenna unchanged. The second assumption is valid for the short lengths of waveguide used within a radar

receiver at the typical operating frequencies of monopulse radars [7:576]. The third assumption is based upon a phone conversation with Mr. Steve Davis of PSI during which Mr. Davis stated that experiments they have performed have confirmed the theory that, with the short duration pulses they were developing, a microwave mixer passed the pulse with minimal spreading of the pulse width [3].

1.8 Equipment Required and Overview of BOSS Software

The BOSS software package provides a complete, interactive simulation environment which allows any engineer familiar with computer simulation theory to perform complex simulations without the need for actually writing the simulation code [2:1.2]. Within BOSS, modules of a basic system are interconnected in a graphical, block-diagram form. The finished system simulation looks very much like a block diagram for the system you might see in any textbook. Once the diagram is correctly configured, BOSS analyzes the component blocks, asks the user for any required operating parameters, and then converts the diagram in a complete FORTRAN simulation program. After the FORTRAN program is run, BOSS allows the user to display the results in a wide variety of output formats. The BOSS software, Version 2.0 by COMDISCO Systems Incorporated, was installed on a Micro-Vax II workstation at AFIT.

1.9 Approach

Analytical models of the various radar components were developed based upon models currently in use in the literature. Two simple amplitude comparison monopulse radar receiver models were implemented using BOSS modules. Once the complete model was developed and implemented using the BOSS software, jam-free input signals were injected into the system and the resulting monopulse ratios were recorded. The model was then modified to reflect various degrees of electrical imbalance between the two channels, and the jam-free signals were again input. This allowed me

to characterize the effect of the receiver mismatch upon the radar's performance. With this information, I was able to determine if the mismatch would have caused significant errors on its own and could therefore have been detected by the receiver's internal fault detection circuits. Next, impulsive jamming signals were added to the input signals and the simulations were repeated. The resulting monopulse ratios were then examined to determine the errors caused by the jamming signals in conjunction with the imbalances within the receivers.

Before the actual models could be developed, a review of the basic methods of extracting the angular information was needed. This information, plus the mathematical models which form the basis of the BOSS simulations is presented next.

II. Amplitude Comparison Monopulse Systems

2.1 Desired Monopulse Characteristics

The basic desirable characteristic of any monopulse processor is that the resulting monopulse ratio should be a linear function of the target angle and should depend upon the ratios of the received antenna patterns, not their absolute values. As Sherman points out, this characteristic is needed so that the monopulse output is dependent upon the *angle* of the target, not on the target's range or radar cross-section [11:153]. The monopulse output should also be an odd function of the angle off of the antenna boresight. This allows the *sign* of the monopulse result to indicate direction. It is also desirable that the monopulse ratio be as linearly proportional to angular displacement of the target as possible. The slope of this linear curve relating target angle to the value of the monopulse ratio is due to the response of the various components in the processor and is designated as K_s . This linearity greatly simplifies the conversion from monopulse output to indicated target angle. Under these conditions, all that is needed to indicate the target's angle is to multiply the result of the monopulse processor by a predetermined calibration constant (basically the inverse of K_s .)

2.2 Antenna Beams Used in Monopulse Radar

The typical monopulse antenna consists of a parabolic reflector fed by four rectangular feed horns centered about the focal point of the reflector. These four horns produce four beams (see Figure 2.1), each offset (or "squinted") an equal amount from the axis of the reflector. If a cross-section of the beams was taken, their corresponding constant potential patterns would appear as in Figure 2.2. These four receive beams are combined at radio frequencies (RF) using a hybrid junction before the signals are input into the receivers. Since the intent of the monopulse receiver is usually to provide angular information along a pair of orthogonal axes, the patterns

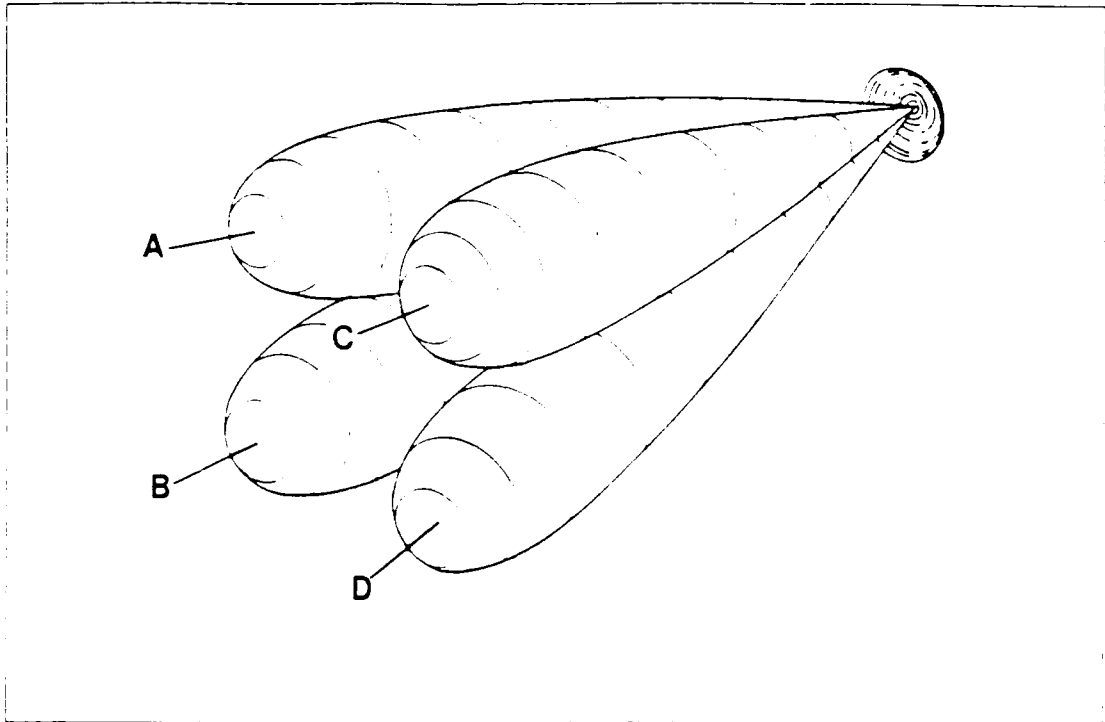


Figure 2.1. The Four Squinted Beams Used in a Typical Amplitude Comparison Monopulse Radar [11:10]

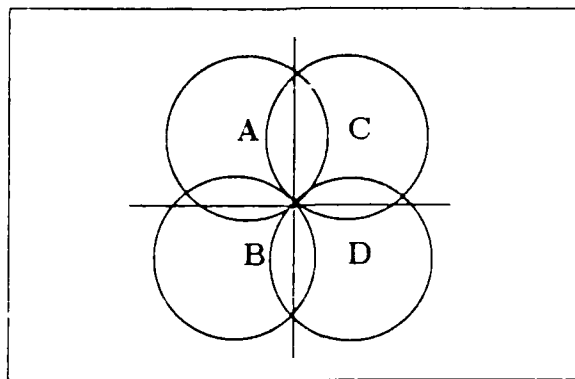


Figure 2.2. The Cross Section of the Four Beams used in an Amplitude Comparison Monopulse Radar [11:11]

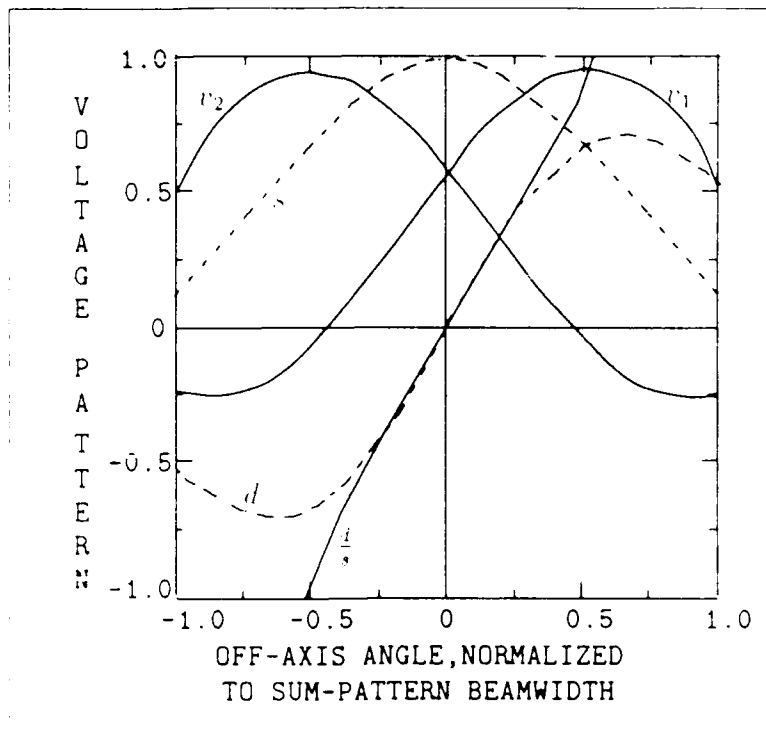


Figure 2.3. Amplitude Comparison Monopulse Patterns in either coordinate: sum (s), difference (d), squinted beams (v_1 and v_2), and the normalized difference ratio ($\frac{i}{s}$). [11:12]

are combined to form a sum pattern and two orthogonal difference patterns

$$s = \frac{1}{2}(A + B + C + D) \quad (2.1)$$

$$d_{\text{azimuth}} = \frac{1}{2}((C + D) - (A + B)) \quad (2.2)$$

$$d_{\text{elevation}} = \frac{1}{2}((A + C) - (B + D)) \quad (2.3)$$

$$(2.4)$$

The result of this combination of patterns is shown in Figure 2.3 for either the azimuth or elevation planes. For the azimuth plane $v_1 = (C + D)/\sqrt{2}$ and $v_2 = (A + B)/\sqrt{2}$ while for the elevation plane, $v_1 = (A + C)/\sqrt{2}$ and $v_2 = (B + D)/\sqrt{2}$. This allows the sum (s) and the difference (d) in each coordinate

to be related to v_1 and v_2 by the following equations

$$\begin{aligned} v_1 &= (s + d)/\sqrt{2} \\ v_2 &= (s - d)/\sqrt{2} \end{aligned} \quad (2.5)$$

Sherman also presents a set of empirical formulas which have been found to be close approximations of the measured s and d patterns of the AN/FPS 16 antenna patterns for the annular region covering most of the main lobe of the sum pattern (the main lobe is approximately 1.1° or 20 milliradians wide) [11:138]; [5:117].

$$s = \cos^2(1.14\theta) \quad (2.6)$$

$$d = \frac{1}{\sqrt{2}} \sin(2.28\theta) \quad (2.7)$$

These equations will be used later to implement the model of the received signal. These s and d functions will be combined as shown in Eq 2.5 and the resulting v_1 and v_2 will form the basis of the signals that will serve as the inputs to the monopulse processor simulations.

2.3 Amplitude Comparison System using Logarithmic Amplifiers

As early as 1950, General Electric Corporation identified the possibility of using amplifiers with logarithmic amplitude responses in a non-coherent processor to determine the monopulse ratio [6:75]. Later, Sherman provided more detail on the configuration of such a system [11:177]. The two input signals consist of components of the sum and difference antenna patterns as shown in Eq 2.5, where v_1 and v_2 are the composite patterns in the plane of interest. In many monopulse RF systems, the actual sum and difference patterns may not be physically represented as voltages anywhere in the receiver, but their information is contained in the developed v_1 and v_2 signals. One must keep in mind that, in a monopulse processor, we are only interested in the ratio of the amplitudes of the sum and difference signals, and therefore any combination

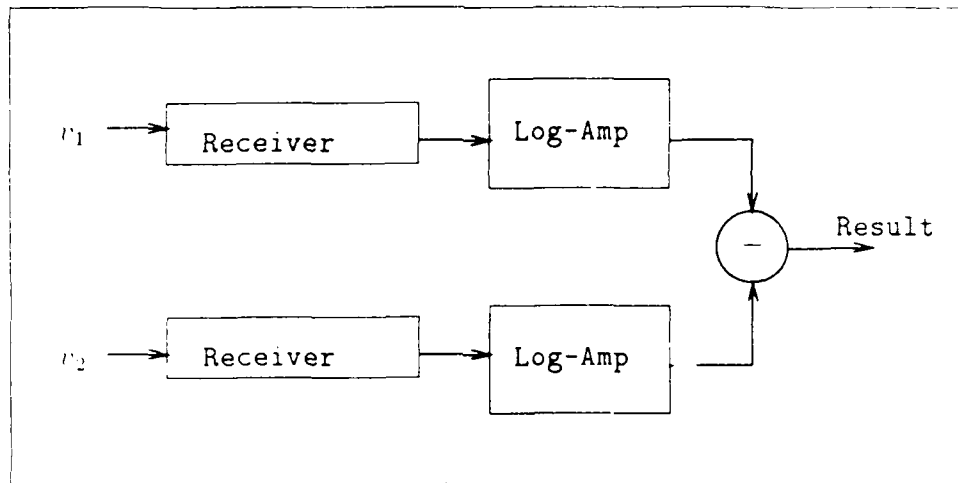


Figure 2.4. Block Diagram of Logarithmic Amplifier Monopulse Processor

[11:178]

of the patterns which maintains this relative relationship can serve as the basis for the extraction of the angular information (see Figure 2.3.) However it is represented, the information in the sum channel is also used to determine the target's range.

Sherman's logarithmic processor (see Figure 2.4) has v_1 and v_2 input into two parallel processing channels. Each channel consists of a receiver feeding an amplifier-detector having a logarithmic response (such an amplifier will hereafter be referred to as a Log-amp.) The output of these Log-amps feed a subtractor. Since $(\ln v_1 - \ln v_2)$ is equivalent to $\ln(v_1/v_2)$, this has the same effect as taking the ratio of the two input signals. The output can be expressed as

$$K_s \ln \left| \frac{v_1}{v_2} \right| = K_s \ln \left| \frac{s+d}{s-d} \right| = K_s \ln \left| \frac{1+d/s}{1-d/s} \right| \quad (2.8)$$

and assuming that $|d/s| \ll 1$ (as shown in Figure 2.3, this is a valid assumption for targets within a quarter beamwidth of the axis of the sum pattern), then

$\ln|1 + d/s| \cong d/s$ and $\ln|1 - d/s| \cong -d/s$. With these conditions met, Eq 2.8 becomes

$$K_s \ln \left| \frac{v_1}{v_2} \right| \cong \frac{2 K_s d}{s} \quad (2.9)$$

which yields the desired monopulse ratio (except for the factor of 2 which can be included in the calibration constant K_s .)

2.3.1 A Log-Amp Model. Leonov presents a mathematical model for a logarithmic amplifier which describes the amplifier response in both the linear and non-linear response modes [9:49]. Using Leonov's model, the log amp response can be described as

$$\begin{aligned} U_{out} &= k_o U_{in} && \text{for } U_{in} < U_{thres} \\ U_{out} &= k_o U_{in} \left[a_l \ln \left(\frac{U_{in}}{U_{thres}} \right) + 1 \right] && \text{for } U_{in} \geq U_{thres} \end{aligned} \quad (2.10)$$

- where U_{in} = input to the amp
- U_{thres} = threshold level input must exceed for logarithmic response
- k_o = gain of amp
- a_l = slope of response curve
- U_{out} = output of logarithmic amp

While Eq 2.10 adequately describes the desired response of a log amp, the compound mathematical expressions make it difficult to implement in a straightforward manner using the basic mathematical BOSS modules. The second expression of Eq 2.10 can be reduced to

$$\begin{aligned} U_{out} &= k_o U_{thres} a_l \ln(U_{in}) - k_o U_{thres} a_l \ln(U_{thres}) + k_o U_{thres} \\ &\text{for } U_{in} \geq U_{thres} \end{aligned} \quad (2.11)$$

which lends itself nicely to a direct implementation using BOSS.

2.3.2 Taking the Natural Log of Complex Value. The input signal U_i in Eq 2.11 can be a complex value, and since BOSS doesn't provide for taking the natural logarithm of a complex number, it was necessary to implement the natural logarithm of a complex number using boss primitive modules. The $\ln(\text{complex})$ function can be expressed equivalently as

$$\ln(x + iy) = \ln |mag| + i \arg(x + iy) \quad (2.12)$$

and since the $|mag|$ is real valued, the \ln is operating only on a real valued quantity.

2.3.3 The Response of the Log-Amp Receiver. To compare the action of this monopulse receiver against that of an assumed *exact* processor, Sherman plotted the response of the Log-Amp processor using a Gaussian beam pattern for the components of the squinted beams v_1 and v_2 and compared it to the response of an exact processor using the same input beams. Sherman describes his proposed *exact* processor as

... one that produces the real part of the complex ratio A/s perfectly for each angle coordinate. This does not mean that such a processor (if it existed) would be better, for every application, than an inexact processor or one designed for a different type of output, but it serves as a reference with which practical processors can be compared [11:158].

Sherman's plot, shown in Figure 2.5, demonstrates the Log-Amp monopulse processor's close approximation to an exact monopulse processor for small values of target angle. One of the primary disadvantages to this type of a receiver is its sensitivity to gain variations between the two channels. A difference in the gains results in a shift of the indicated null of the antenna patterns. This shift in the nulls is proportional to the gain difference. To illustrate this, assume that the gain in the v_1 channel is

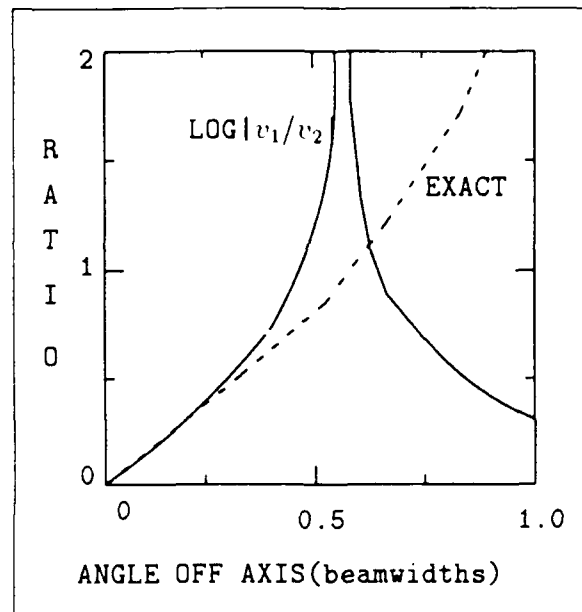


Figure 2.5. Outputs of $\ln |v_1/v_2|$ Processor and Exact Processor vs Angle [11:180]

given by K_1 and the gain in the v_2 channel is K_2 , and that $K_1 \neq K_2$. The expression given in Eq 2.8 can be expressed as

$$K_s \ln \left| \frac{K_1 v_1}{K_2 v_2} \right| = K_s \left| \frac{v_1}{v_2} \right| + K_s \ln \left| \frac{K_1}{K_2} \right| \quad (2.13)$$

which will induce an offset of $K_s \ln |K_1/K_2|$ in the output of the monopulse ratio, and would translate into an equivalent offset in the indicated target angular position.

2.4 Automatic Gain Control in Monopulse Radars

A radar receiver must be able to process a very wide range of signal amplitudes. In the Log-Amp system (see Figure 2.4), the dynamic range of the input signal is accommodated using amplifiers with a logarithmic response. Another method of providing this dynamic range is to use automatic gain control (AGC) to adjust the amplitude of the incoming signal to the desired value. The primary goal of any AGC circuit is to adjust its output to within a certain, narrow band of amplitudes. There

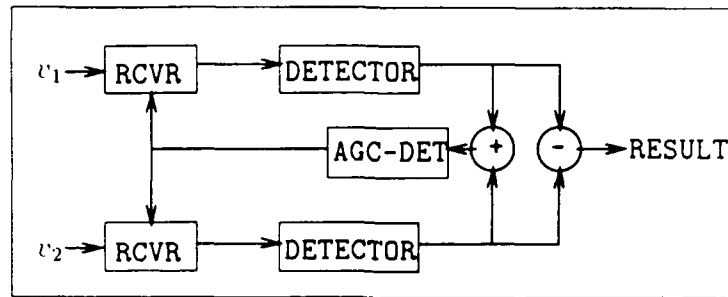


Figure 2.6. Block Diagram of Monopulse Processor using AGC [11:173]

are two common types of AGC discussed in radar literature, *instantaneous* AGC (IAGC), and *slow* AGC. IAGC is able to respond very quickly to changes in the input, and has response times that are generally less than thirty to fifty pulse-widths in duration while Slow AGC has a response considerably longer than this [8:313]. In addition to providing the needed dynamic range for the receiver, IAGC can be used in monopulse receivers to reduce the circuitry needed to extract the monopulse ratio. Since the AGC used in monopulse processors is normally IAGC, I will use the term AGC to refer to IAGC response systems from here on.

2.5 An AGC Based Monopulse Processor

Sherman outlines the basic components of an AGC based processor, and the one that is presented here is based upon his Figure 7.10-1 (Sherman refers to it as a Noncoherent Processor using the sum and difference of $|v_1|$ and $|v_2|$.) He describes a modification to this system which eliminates the need for the addition and division blocks, and this modified system is used as my AGC-Type monopulse processor [11:173].

By using an AGC signal based upon $|v_1| + |v_2|$ to control the gain of the amplifiers in both channels, the output of the subtractor ($|v_1| - |v_2|$) is, in effect, normalized by $(|v_1| + |v_2|)$. Since the relative phase of the two channels is the

same, the absolute value signs can be omitted, and the result achieves the desired monopulse ratio

$$\frac{|v_1| - |v_2|}{|v_1| + |v_2|} = \frac{v_1 - v_2}{v_1 + v_2} = \frac{(s + d) - (s - d)}{(s + d) + (s - d)} = \frac{d}{s} \quad (2.14)$$

2.5.1 An AGC Model. A model of an AGC system is briefly described by Hughes [4:14] and is also described in great detail by Leonov [9:69-73]. Under the assumptions of a linear receiver, Leonov showed that the behavior of the AGC system could be described by

$$U_{out} = k_m U_{in} \quad \text{for} \quad U_{out} < U_d \quad (2.15)$$

$$U_{out} = k_c U_{in} \quad \text{for} \quad U_{out} \geq U_d \quad (2.16)$$

where the AGC control voltage (k_c) is described by

$$k_c = b_a U_c \quad (2.17)$$

$$U_c = k_f F_a(p)(U_{out} - U_d) \quad (2.18)$$

with the following definitions:

- k_m = max gain with no AGC control
- U_{in} = the input signal
- U_d = the *delay* or desired voltage
- b_a = the response of the AGC amplifier in db/Volt
- U_{out} = output

$$\begin{aligned}
U_c &= \text{the AGC control voltage} \\
k_f &= \text{the gain of the feedback loop} \\
F_a(p) &= \frac{1}{(pT_a+1)} \text{ the feedback filter response} \\
T_a &= \text{the filter time constant}
\end{aligned}$$

This model is easily implemented using BOSS modules. The AGC circuit should be updated only during the time of the range gate [11:155]. The AGC output from one pulse is applied to the next received pulse.

Hughes describes the interaction between the choice of time constants for the low-pass filter in the feedback loop and the PRI of the received signal [4:15]. The effective time constant of the feedback filter is given by

$$T_{pulse} = RC \left(\frac{PRI}{T_u} \right) \quad (2.19)$$

where T_u is the time the AGC circuit is updated. Using this relationship it is possible to increase the effective time constant of the AGC detector by either changing the corner frequency of the filter or by increasing the PRI.

2.5.2 The Response of the AGC Based Processor. Once again, Sherman plotted the response of an AGC based processor against that of an assumed *exact* processor. This time, he used the antenna patterns of an AN/FPS-16 radar system as the inputs. As Figure 2.7 shows, the two processors have identical outputs up to the point where the output equals 1. At angles greater than the angle which corresponds to this point, the magnitude of the output of the AGC-Type processor is ambiguous. In a null-tracking, monopulse radar the target is kept near the null of the antenna by the antenna tracking mechanism. In the acquisition mode (during which the target may be offset significantly from the antenna's boresight), although the magnitude of the indicated target angle may be ambiguous, the *sign* of the output will still indicate the correct direction of the target. The tracking loops will drive the antenna toward the target until the target is within the unambiguous region.

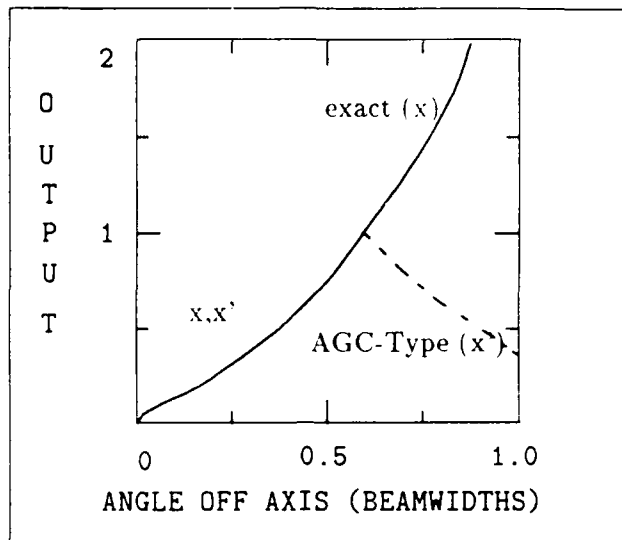


Figure 2.7. Outputs of an *Exact* and an *AGC-Type* processor, as a function of Target Angle [11:175]

This processor, like the Log-Amp type processor, is susceptible to shifts in the indicated antenna boresight when the two channels have different gain values. This dependence upon the equality of the two channel's gains can be shown by introducing a gain constant for each channel as was done in the section on Log-Amp response. Let the total gain of the v_1 channel be K_1 and v_2 channel's gain be K_2 . Then, Eq 2.14 becomes

$$\frac{K_1 v_1 - K_2 v_2}{K_1 v_1 + K_2 v_2} = \frac{K_1(s + d) - K_2(s - d)}{K_1(s + d) + K_2(s - d)} \quad (2.20)$$

which, after separating the numerator and rearranging, can be expressed as

$$\frac{(K_1 - K_2)s}{(K_1 + K_2)s + (K_1 - K_2)d} + \frac{(K_1 + K_2)d}{(K_1 + K_2)s + (K_1 - K_2)d} \quad (2.21)$$

At angles near the boresight of the antenna, the difference antenna pattern of Figure 1.1 (b) has a voltage pattern near zero amplitude when compared to the sum pattern voltage. Assuming that the degree of gain imbalance between K_1 and K_2 is

small and that $(K_1 - K_2)d \ll (K_1 + K_2)s$, the expression given in 2.21 becomes

$$\frac{(K_1 - K_2)s}{(K_1 + K_2)s} + \frac{(K_1 + K_2)d}{(K_1 + K_2)s} = \frac{d}{s} + \frac{K_1 - K_2}{K_1 + K_2} \quad (2.22)$$

which demonstrates the nature of this mismatched gain responses of the two channels.

The mathematical models presented in this chapter formed the basis for the BOSS modules described in the following chapter.

III. BOSS Implementation of System Models

3.1 Overview of Model Implementation on BOSS

With its graphical interface, BOSS makes the development of complicated simulations very straightforward. One of the original authors of BOSS, Shannugan, describes the user interaction with BOSS:

BOSS assumes that modules, subsystems and systems (whether they are control systems, communication systems or signal processors) can be represented in a hierarchical block diagram form. Module construction and specification is designed around an interactive, graphic Block Diagram Editor (BDE). A high resolution graphics terminal is used to display, edit and interact with the BDE.

The engineer uses the BDE to construct a block diagram of the module, sub-system or system to be simulated. The BDE encourages a hierarchical, *bottom-up design approach*. . . Initially, the engineer is provided with a set of primitive modules, such as adders, multipliers and comparators. The engineer then connects the selected modules together with signals and provides required parameters and documentation [10:36.1.2].

A complex model can be saved in BOSS and later used as if it were a primitive module; it will appear on the screen as a small rectangle with only the name and the input/output pads. In this manner a complex system can be built from a series of complicated sub-modules, without the top-level simulation block diagram appearing too complicated.

Prior to running a simulation, BOSS allows you to place "probes" at any of the input or output pads in the system. The probes collect data during the simulation and can be used to display the results of the simulation. BOSS also allows you to display results by feeding the desired signal into one of several types of Tabular Data Plot Accumulators¹ which display results in an x-y data plot.

¹Sans-Serif type will be used throughout to refer to a module as it is labeled within BOSS

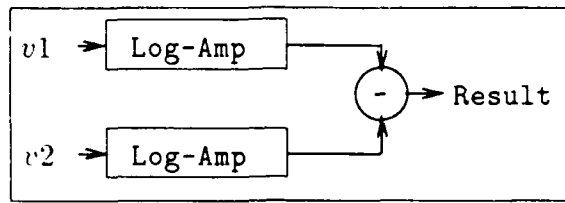


Figure 3.1. A Simple Log-Amp Model

Before BOSS can actually run a simulation, the user is prompted for all of the necessary parameters. BOSS then generates the FORTRAN code corresponding to the desired system simulation. It is this self-contained FORTRAN program which actually performs the simulation.

3.1.1 An Example of a BOSS Simulation. To illustrate the methodology behind creating a simulation using BOSS it is best to follow a simple example from start to finish. A model of a simple Log-Amp monopulse processor is presented by Sherman (see Figure 3.1), and it is desired to implement this model using BOSS [11:178]. The inputs to the two channels ($v1$ and $v2$) would come from another BOSS module which simulates the signals from the RF front-end of the receiver and provides its results at the output pads. The output pads of this module would be connected to the input pads of the Log-Amp module.

The subtractor shown in Figure 3.2 is available as a primitive module, so it can be selected from the available module menu. An empty rectangle representing the subtractor module appears, and using the mouse, can be placed anywhere on the display. Since BOSS doesn't provide a Log-Amp as a primitive module, it will have to be implemented using primitive modules interconnected to conform to a mathematical model of a Log-Amp. Assuming that this was done previously, then the rectangle representing the Log-Amp module can be manipulated just like the primitive module of the subtractor. The output of the subtractor must go somewhere,

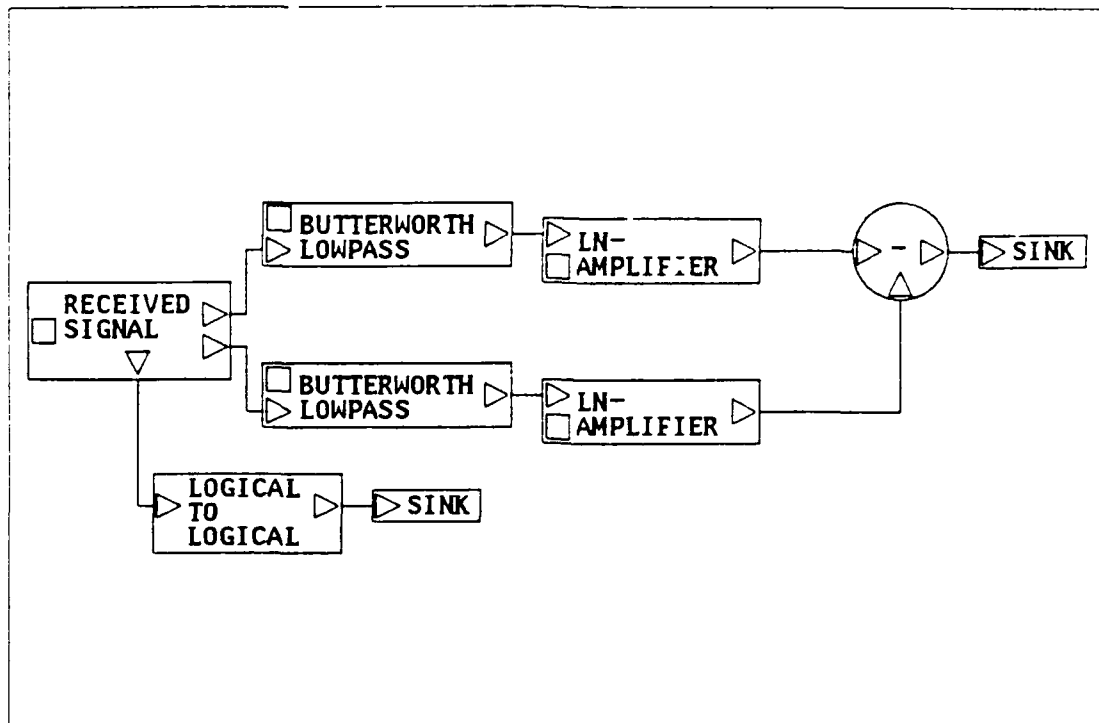


Figure 3.2. BOSS Implementation of the Simple Log-Amp Model

and since the subtractor output is our desired result, it can feed a “sink” module (we can attach a probe later.) The third output of the Received Signal Generator block is not needed here, but since BOSS insists that every output and input pad be connected this output feeds another “sink” module.

Once all of the input and output pads of all modules have been correctly interconnected, then the module can be saved as a complete simulation model. Prior to saving the model, you have the option of explicitly stating the value of any simulation parameters or exporting them as external parameters to be specified later. This ability to export parameters allows you to have a parameter from a small module which is used within a larger module (or complete system) and not specify the parameter’s value until the simulation is run. If a parameter is not exported, but is explicitly defined, then it no longer is available as a variable to the next higher

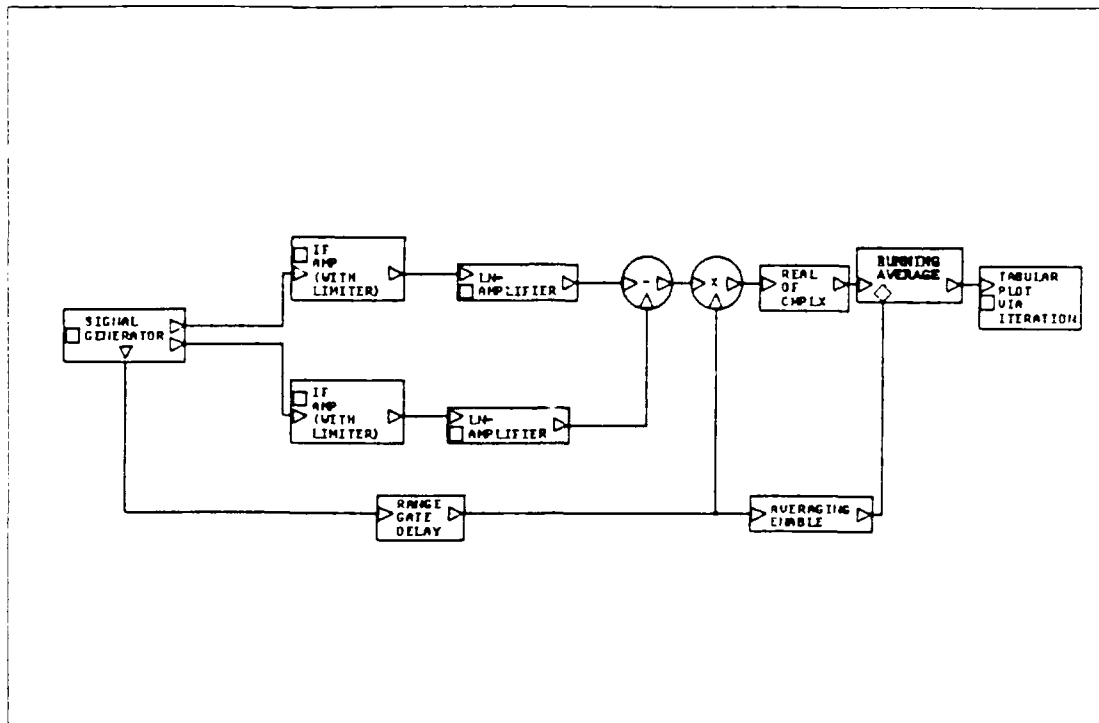


Figure 3.3. The Log-Amp System as Modeled in BOSS

module. BOSS does an excellent job of checking parameter declarations, types, and limits to ensure compatibility among modules. For example, BOSS won't allow you to connect a "complex" output pad to a "logical" input pad, or a "real" output with a $\pm\infty$ limit to an input pad with a ≥ 0 limit.

After BOSS performs the simulation, the results are available through the Post-Processor menu of BOSS. The Post-Processor offers a wide variety of options for the display of the data collected during the simulation. Data can be examined from a time-domain or a frequency domain perspective.

3.2 A Log-Amp Monopulse Processor Model in BOSS

The Log-Amp processor discussed in section 2.3.1, was implemented in BOSS as shown in Figure 3.3. It is composed of BOSS primitive modules and sub-modules

which were constructed separately.

3.2.1 BOSS Primitive Modules Used. The presentation of the model will begin with a discussion of the modules which were available as BOSS primitive modules. To keep the simulation times reasonable, all simulations will be performed at video. The IF Filters which are actually bandpass filters at the IF frequency, can be modeled as 3rd order **Butterworth Lowpass Filters** at video, and their parameters expanded to allow the specification of the *corner frequencies prior to each simulation run*. The filter outputs are limited to ± 12 volts to account for power supply limitations in an actual receiver.

The **Range Gate Delay** module is actually another BOSS module, the **Multi-Stage Delay**, renamed to reflect its use within the model. The amount of delay time is adjusted (based upon an examination of the time domain behavior of the IF filter's output) to center the range gate over the output of the IF filters.

The **Subtractor (-)** and **Multiplier (x)** modules allow inputs of either complex or real signals (naturally both inputs must be of the same type.) The **Real of Complex** module is one of several modules BOSS provides for separating complex signals into their components. In this instance, since we are modeling a non-coherent system, only the real component of the signal is needed. The signal must be kept in its complex form up to this point however, as the **Butterworth Filter** modules only accept complex input signals.

The **Running Average** module computes the average of its input signal over each **sample period** that it is enabled by the enable signal at the "diamond" shaped input pad. Any input to this module at any other time does not get included in the average.

The **Tabular Data Plot via Iteration** module collects the input data and plots it on a two-axis plot. The vertical axis is the result of the simulation, and the horizontal axis is based upon a parameter which is incremented by a predefined amount for a

variable number of iterations. This allows the results of several simulations, each identical except for the one parameter which is incremented, to be displayed on one plot. This type of data gathering is an excellent method of demonstrating a simulation model's dependence upon one parameter. For this model, the "angle off boresight" parameter (used in the **Received Signal Generator** module and discussed below) is varied from one side of the antenna centerline to the other.

The **Averaging Enable** module contains one of BOSS's "types" or "units" conversion modules, **Real of Complex** which takes the real portion of the complex signal from the **Range Gate Delay** module (either a (0.0) or a (1.0)). This real component is then compared to a constant value of "1" using a **>=Real** module. The result of this comparison yields a logical "true" or "false" depending upon the state of the range gate delay signal. This logical signal is then used to "enable" modules which should only execute during the range gate enable period.

3.2.2 Modules Built from Primitive Modules. Three of the modules, the **Received Signal Generator** and **LN-Amplifier**, and the **Complex-LN**, are actually more complex BOSS modules which were constructed and saved separately and then used as if they were provided by BOSS as primitive modules.

3.2.3 The Received Signal Generator. The **Received Signal Generator** model implements the mathematical expression for the v_1 and v_2 signals as developed in section 2.2 and also forms the desired pulse width and pulse repetition frequency (PRF), adds any random noise needed to establish a specifiable signal-to-noise ratio (SNR), and allows an impulse to be superimposed at a specified time on the signal train to simulate an impulsive jammer.

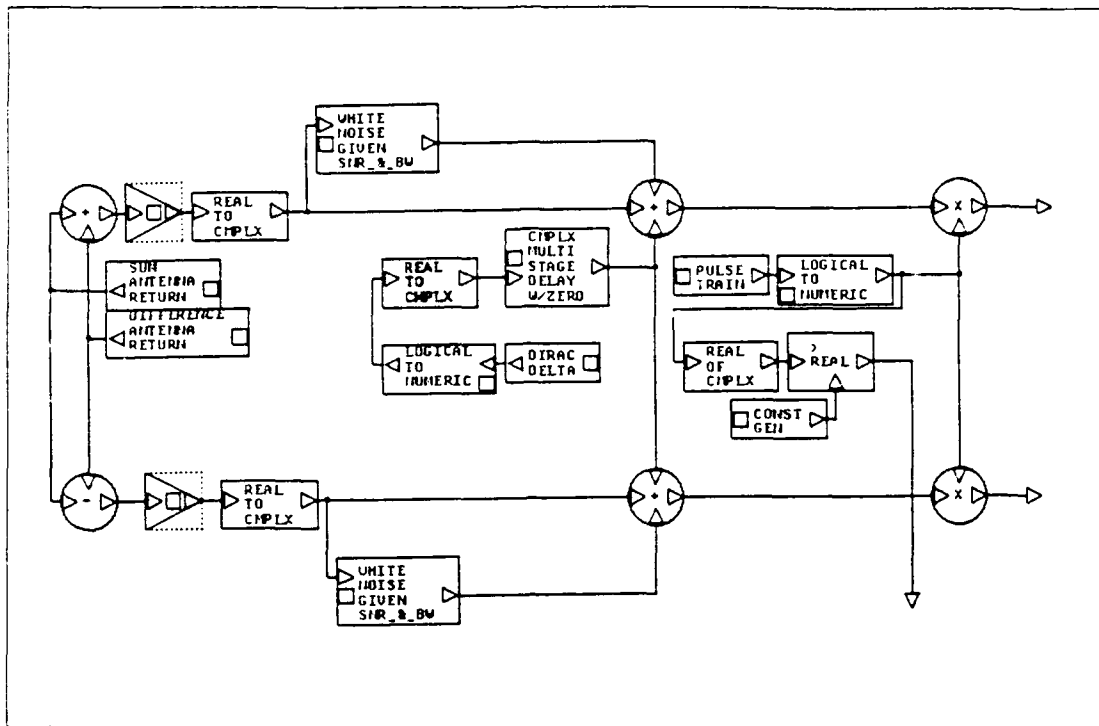


Figure 3.4. The BOSS Received Signal Generator Module

The description of this module will follow the signal path as if the signal were moving from the left to right in Figure 3.4. The Sum Antenna Return and Difference Antenna Return modules are Analog Constant Generator modules with the "constant" parameter set equal to the appropriate formula given in either Eq 2.6 or Eq 2.7. The angle variable θ was exported under the name "Angle off boresight" and is the parameter that is incremented during the simulations to reflect the signal's return as a single target moves from one side of the antenna boresight to the other. The output of the Analog Constant Generators is indeed constant for each discrete value of θ , but θ is incremented for each iteration in the total simulation. The v_1 or v_2 signal is formed by adding or subtracting (as appropriate) the outputs of these two modules. The gain modules provide an adjustable scale factor for the overall signal strength.

Since the **White Noise Given SNR_&_BW** modules must have complex input signals, the signal must first pass through a **Real to Complex** conversion module. The **White Noise Given SNR_&_BW** modules allow for the specification of a desired SNR for a given signal bandwidth (the bandwidth is set to equal to the simulation bandwidth $2/d_t$ with d_t equal to the time between samples in the simulation.)

Next, the **Dirac Delta**, provides a logical "true" for one simulation interval (d_t) at the desired time. During the simulation, the model's response to several pulses will be examined and the response to an impulse may be a function of when the impulse is applied during a train of signal pulses. For this reason, the time parameter of the **Dirac Delta** module is adjusted to correspond to the leading edge of the desired pulse. The position of the impulse within the desired signal pulse is specified in terms of a delay from the rising edge of the pulse via the **Complex Multi Stage Delay W/Zero** module.

The **3-Input Adder** modules are used to combine the pure signal, the noise component, and the jamming impulse into a composite signal prior to passing the signals to a multiplier which acts as an "on/off" switch to develop the desired signal pulse train.

The multiplier is fed by a **Pulse Train** module which allows for the specification of a desired pulse width and PRF. The **Pulse Train** module's output is a logical signal, alternating between +1 and -1 logic levels, and so must be converted to a complex signal type before it can be applied to the multiplier. The **Logical to Numeric** module accomplishes this, converting the ± 1 logical signal to a (1,0) signal during a logical +1 and a (0,0) signal during a logical -1. This complex signal also serves as the basis for the range-gate signal and is made available to other modules via an output pad, as is the final form of the pulse train.

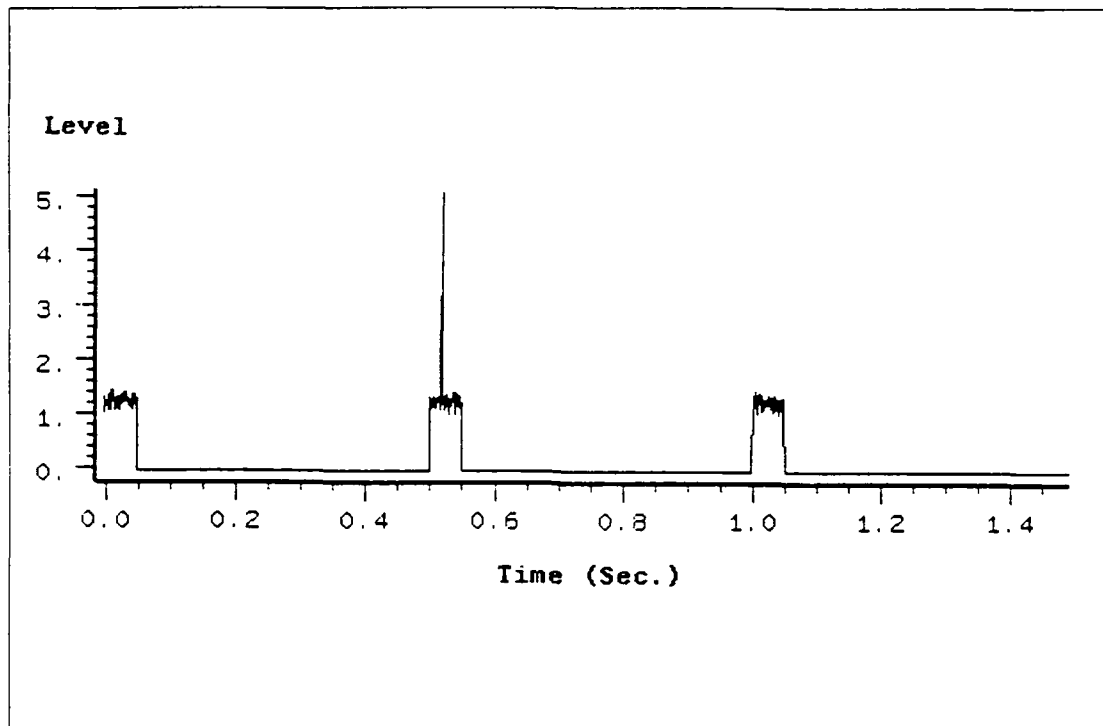


Figure 3.5. An example of the Output of the Received Signal Generator module

An example of the output of this module is shown in Figure 3.5 for a pulse train with a pulse width of 0.05 seconds, a PRF of 2Hz, 20dB SNR, and the impulse applied with a delay of 0.02 seconds into the second pulse. This is not a true time scaling of a representative radar pulse (i.e. the PRF is not scaled the same as the pulse width); however, the impact of this particular choice of PRF was discussed in Section 2.5.1.

Figure 3.6 is a plot of the normalized magnitude of the output of the Received Signal Generator module (without any noise or impulses applied) as the parameter "Angle off Boresight" is varied from -8 milliradians to $+8$ milliradians. Since the equations used in the module were valid for angles near the center of the sum beam of the AN/FPS-16 radar (which is about 20 milliradians wide), this plot gives a fairly accurate indication of the relationship between the v_1 and v_2 signals in the

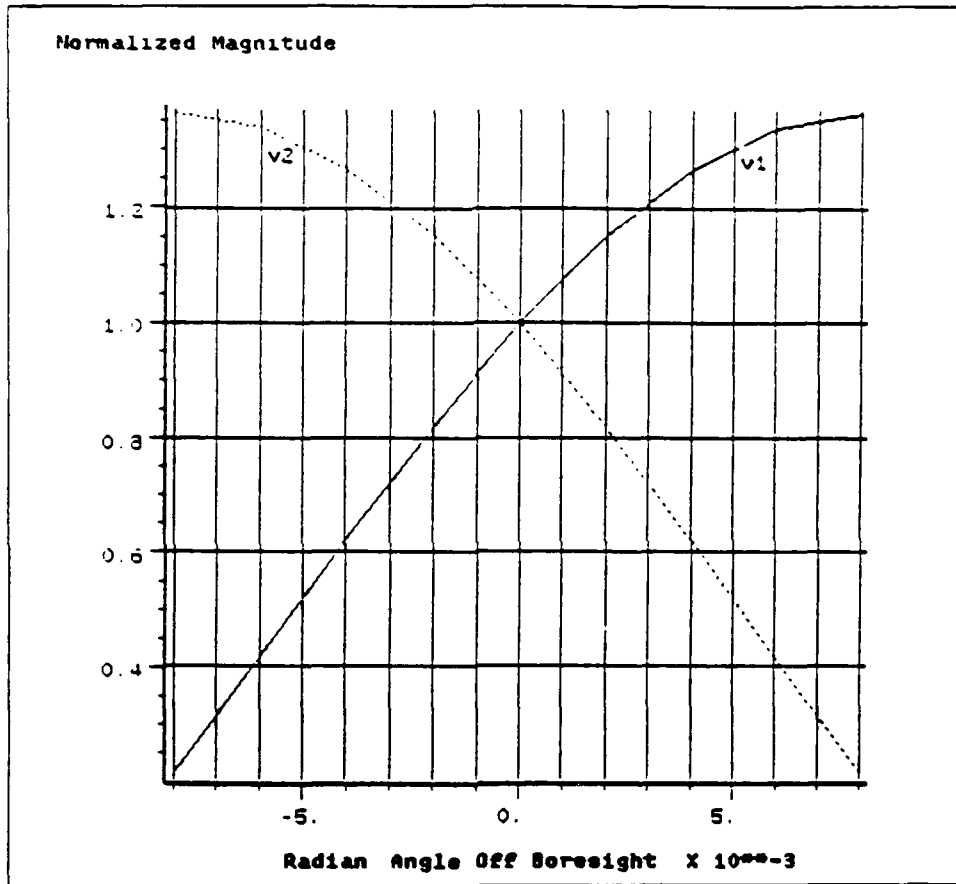


Figure 3.6. The output of the Received Signal Generator module showing the relationship of v1 to v2 as the "Angle off Boresight" parameter is varied from -8 milliradians to +8 milliradians

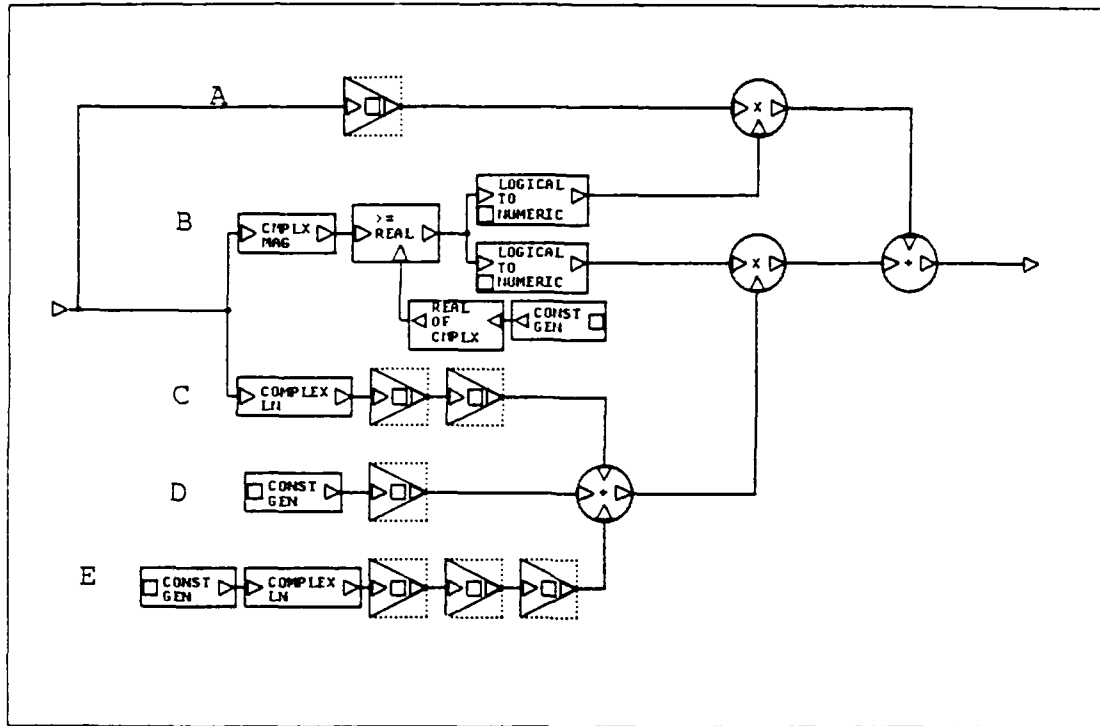


Figure 3.7. BOSS Implementation of the Log-Amp

area from -4 milliradians to $+4$ milliradians.

3.2.4 *The LN-Amplifier Module.* The Log-Amp was implemented using the equations presented in Section 2.3.1 and is shown in Figure 3.7. With the exception of the Complex LN sub-module, the LN-Amplifier module was constructed entirely of BOSS primitives. The description of this module will follow a left-to-right, top-to-bottom pattern.

The top signal path (labeled "A") provides the linear gain response of the Log-Amp for signals which do not exceed the threshold level. The two multiplier modules act as switches to select either the linear or logarithmic responses, based upon the action of the threshold detector in path "B".

The desired threshold level is an exported parameter. The threshold is specified

as a complex quantity since it will be used in its complex form later. The magnitude of the threshold and the input to the LN-Amplifier are compared and a conversion of the "logical signal type" result to a "complex signal" is made. If the magnitude of the input signal exceeds the threshold value, then a complex value of (0,0) is applied to the top multiplier to disable the linear response path "A". At the same time, a (1,0) is applied to the second multiplier switch to allow the results of the logarithmic response paths (C, D, and E) to pass to the two-input adder just prior to the output pad. This final adder will have either the linear path results *or* the logarithmic path results, *but not both*, applied to it at any one time. For input magnitudes less than the desired threshold level, the conversion of the logical result is reversed, allowing the linear path "A" to pass to the output while shutting off the logarithmic channel.

Paths "C", "D" and "E" provide the actual logarithmic response as described in Eq 2.11. Each path performs one of the three components of the equation. Although it would have been possible to reduce the number of modules needed by combining functions, this direct implementation was chosen to make the equality with Eq 2.11 obvious. The amplifier modules in each path provide the gain k_o with the final amplifier in path "E" inverting the results of that path (in order to perform the subtraction needed) prior to the addition of all three paths.

3.2.5 The Complex-LN Module. Since BOSS does not provide for taking the natural logarithm of a complex value, this function had to be synthesized using the equivalent expression of Eq 2.12. As Figure 3.8 shows, it was a simple matter to implement the complex-ln function using BOSS. The complex input signal is split into its magnitude and phase components and then recombined into a complex signal using a module (**Make Complex**) which requires its inputs be in the form of Real and Imaginary components. The natural log of the magnitude of the complex signal becomes the Real component and the phase of the complex becomes the imaginary input. The enable signal is used to prevent an error from attempting to calculate the natural logarithm when the magnitude is zero.

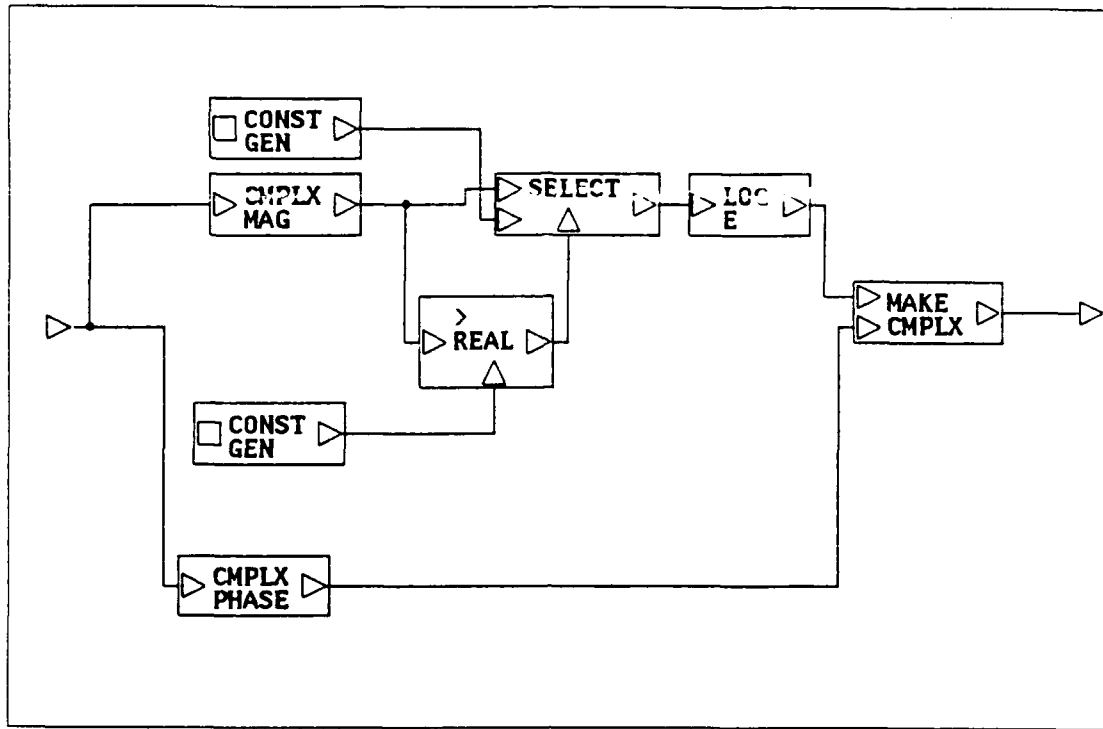


Figure 3.8. BOSS Module to take Natural Logarithm of Complex Signal

3.2.6 *Definition of Angular Error.* For this thesis, angular error is defined as

$$\theta_{err} = \theta_{model} - \theta_{target} \quad (3.1)$$

where θ_{model} is the output of the model for an input signal corresponding to a target located at θ_{target} . Also, targets to the right of the boresight axis are defined as those which result in a positive monopulse ratio output, while a negative monopulse ratio will represent targets to the left of the axis of the antenna.

The concept of an induced angular error can best be understood by examining the d/s curve of Figure 2.3. If this curve was the output of our monopulse processor, the vertical axis would correspond to the magnitude of the monopulse ratio. To find the angle of a target based upon the magnitude of the monopulse ratio, this ratio

must be multiplied by a calibration constant which will yield the angle. As was stated in the opening paragraph of Chapter 2, this calibration constant is basically the inverse of the slope of the monopulse ratio curve. Once the constant is calculated for a given system, any imbalances in the system which might disturb the magnitude of the output of the processor will cause an error in the indicated target angle.

As an example, if a target was located at a normalized angle of +0.25 beamwidths in Figure 2.3, the output of the calibrated processor would be approximately 0.4. If an imbalance in the processor was to cause the output to be reduced in magnitude to say, 0.25, then using the original calibration constant this would indicate that the target was located at a normalized off-axis angle of 0.15 beamwidths. This shift to the left of the actual target would then correspond to an induced angular error of $(0.10 - 0.25)$ or -0.10 beamwidth error.

One must pay careful attention to the sign of the angular error relative to the location of the target. A negative angular error would cause the indicated target location to move *toward* the boresight axis if the target was to the right of the axis but would cause the indicated target to move *away* from the axis if the target were to the left of the boresight axis.

3.2.7 The Log-Amp Angular Error Model. The model of the Log-Amp system presented above has the monopulse ratio as its output. While the behavior of this ratio can give considerable insight into the nature of the model's response for various configurations, it doesn't provide a direct method to evaluate the angular errors due to imbalances of either the gains or frequency responses of the two parallel processing channels. The model shown in Figure 3.9 has this angular error as its output. To conform to the definition established in Eq 3.1, the output of a complete Log-Amp model with balanced gains and frequency response is subtracted from the model under test. This gives Δ_{ratio} which is then divided by the slope of the balanced model's monopulse ratio to yield the angular error. The blocks labeled **Test System**

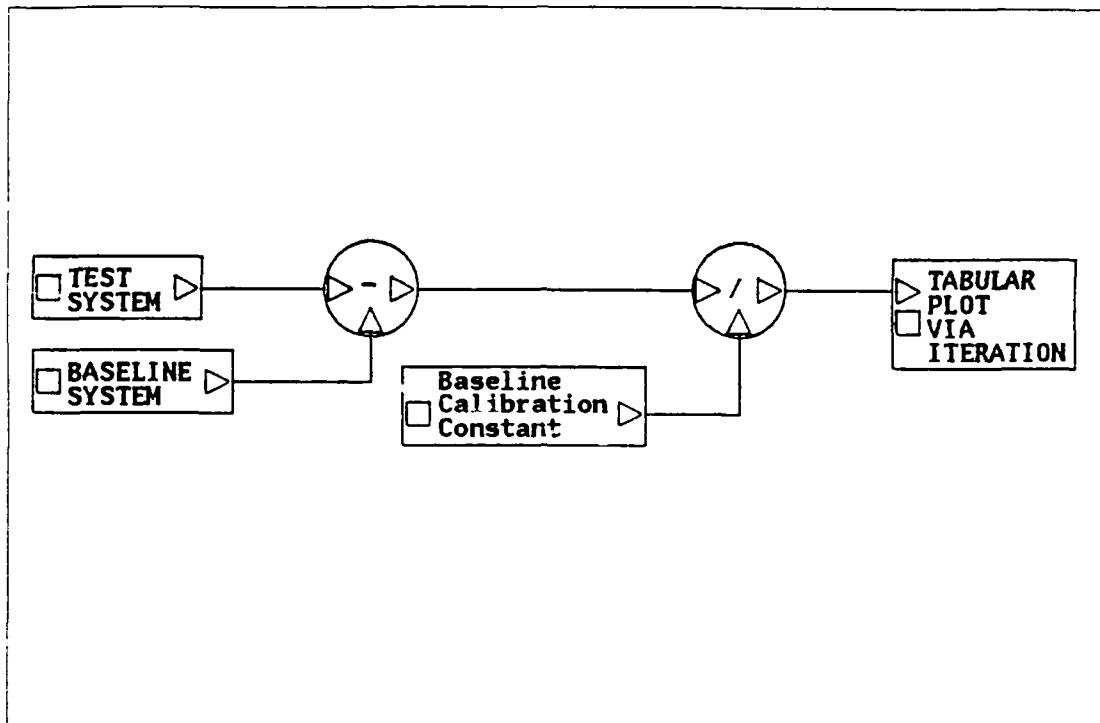


Figure 3.9. A Boss Model to Compute Induced Angular Errors

and Baseline System are complete Log-Amp Modules as shown in Figure 3.3 with the plot accumulator removed.

3.2.8 Parameters Used in the Log-Amp Models. The parameters used within the Log-Amp model were either specified or exported to the final simulation level as shown in Table 3.1. Values which did not need to be varied between simulation runs were specified prior to saving the overall model in BOSS. The parameters which were to be varied in order to explore the action of the model in different configurations were exported to the top layer of the simulation, where they were specified immediately prior to each simulation.

Table 3.1. The Significant Parameters Used in the Log-Amp System Simulations

Parameter	Sub-Module Used in	Set To	Exported As
SNR	Received Signal Generator	-	real
Noise On-Time	Received Signal Generator	-	seconds
Impulse Delay	Received Signal Generator	-	seconds
Pulse Rate	Received Signal Generator	-	Hz
Impulse Time	Received Signal Generator	-	seconds
Impulse Peak Power	Received Signal Generator	-	watts
Angle Off Boresight	Received Signal Generator	-	milliradians
Pattern Factor	Received Signal Generator	7.0711^{-9}	-
V1 LN-Gain	LN-Amplifier in V1 Channel	-	complex
V2 LN-Gain	LN-Amplifier in V2 Channel	-	complex
V1 Filter Edge Freq.	LN-Amplifier in V1 Channel	-	Hz
V2 Filter Edge Freq.	LN-Amplifier in V2 Channel	-	Hz
LN-Threshold	LN-Amplifiers (both)	$(10^{-9}, 0)$ volts	-
Calibration Constant	Angular Error Model	-	real

3.3 The AGC-Based Monopulse Processor as Modeled in BOSS

The AGC based processor discussed in Section 2.5.1 was implemented in BOSS as shown in Figure 3.10. Several modules are the same as those used in the Log-Amp Model (see Figure 3.3.) The Received Signal Generator, Range Gate Delay, IF Filters, Averaging Enable, Running Average, and Tabular Data Plot via Iteration are the same modules as described earlier.

3.3.1 The General AGC Loop Modeled The AGC used in this model is a closed loop AGC system. In its simplest form, the outputs of the two IF amplifiers feed the into the AGC detector which sums the two inputs and then passes them through a low-pass filter. The output of the low-pass filter is amplified and is converted into a gain control signal which adjusts the gain of the input into the IF amplifiers, thus completing the loop.

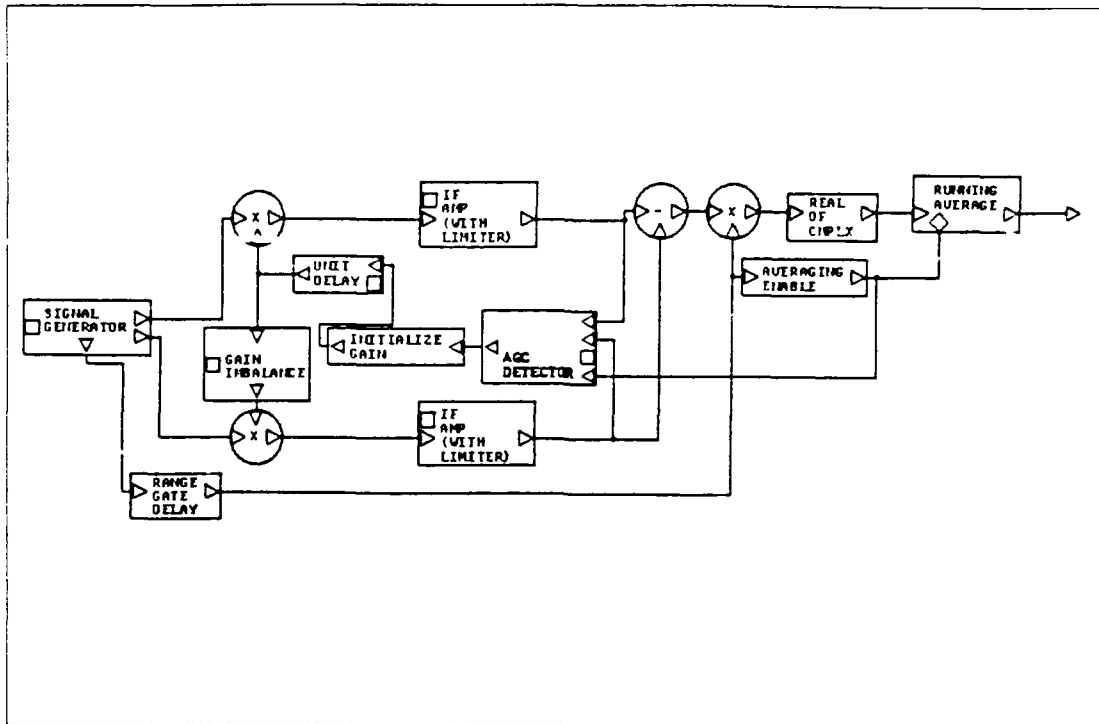


Figure 3.10. The AGC-Type Monopulse Processor as Modeled in BOSS

3.3.2 *Specific AGC Design Parameters* In his book on AGC uses in radar applications, Hughes provides a complete set of design equations for a low-pass filter based AGC detector [4:5-16].

Most IF amplifiers exhibit a linear relationship between AGC control voltage and the amplifier's gain in dB. These design equations will be used to realize an AGC system which has the characteristics shown graphically in Figure 3.11 and given mathematically as

$$A_{IF} \text{ dB} = A_o \text{ dB} - X(\text{AGC Voltage}) \quad (3.2)$$

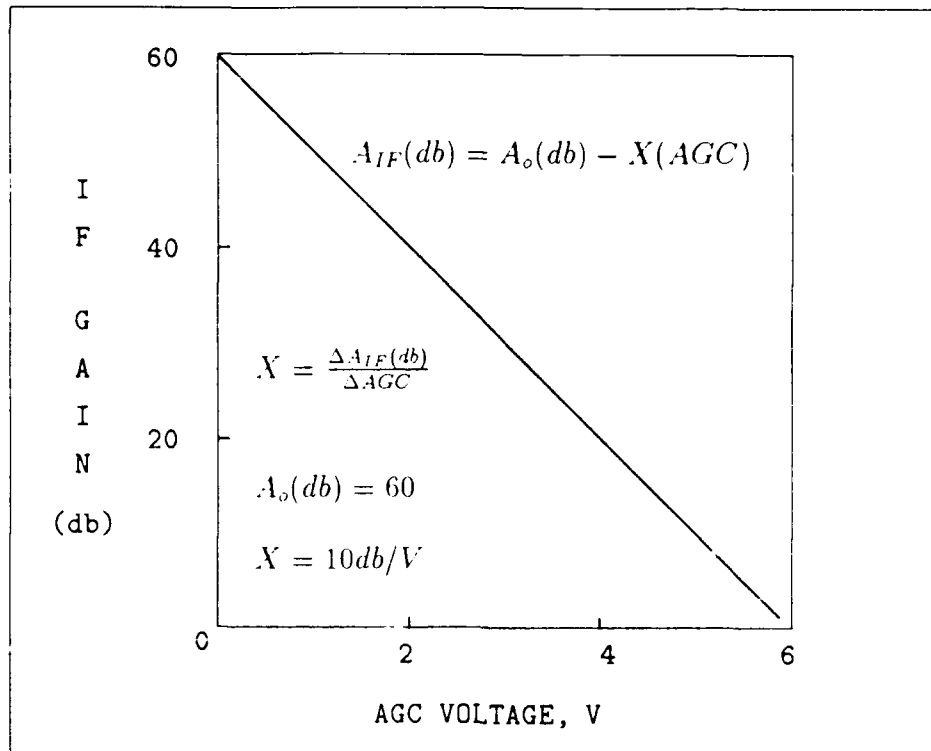


Figure 3.11. Desired Response of IF Amplifier to AGC Voltage

Hughes develops two equations which can be used to solve for the desired feedback gain (A_f) based upon a specified input dynamic range (ΔP_{in}) and amount of regulation desired (ΔP_{IF}) [4:11].

$$LG_{in} = 0.115 \left| \frac{\Delta P_{in}(dB)}{\left(10^{\frac{\Delta P_{IF}(dB)}{20}} - 1\right)} \right| \quad (3.3)$$

$$LG_{in} = 0.115 X A_{\Delta} A_c e_n \quad (3.4)$$

with the following definitions:

- LG_{lin} = Loop Gain (linear detector)
- ΔP_{in} = Input Dynamic Range
- ΔP_{IF} = Output Dynamic Range
- $A_{\Delta}A_e$ = Gain of components in feedback loop
- X = Slope of IF Gain versus AGC voltage (Figure 3.11)
- ϵ_n = normalized video voltage

For a desired input dynamic range of 50 dB (from -70dBm to -20dBm) and output dynamic range of 1 dB, Eq 3.3 becomes

$$LG_{in} = 0.115 \left| \frac{\Delta P_{in}}{(10^{\frac{1}{20}} - 1)} \right| = 47.125 \text{ dB} \quad (3.5)$$

Setting $\epsilon_n = 1$ and combining $A_{\Delta}A_e$ into a single gain A_f and using the value of X from Figure 3.11, Eqs 3.3 and 3.4 become

$$47.125 = 0.115 X A_f \quad (3.6)$$

$$A_f = \frac{47.125}{0.115} 10 = 40.97 \approx 41 \text{ dB} \quad (3.7)$$

Making the appropriate substitutions, Eqs 2.15 to 2.18 become

$$U_{out} = 60 U_{in} \quad \text{for} \quad U_{out} < U_d \quad (3.8)$$

$$U_{out} = k_c U_{in} \quad \text{for} \quad U_{out} \geq U_d \quad (3.9)$$

with the AGC control voltage (k_c) described by

$$k_c = X U_c = 10 U_c \quad (3.10)$$

$$U_c = A_f F_a(p)(U_{out} - U_d) = 41 F_a(p)(U_{out} - U_d) \quad (3.11)$$

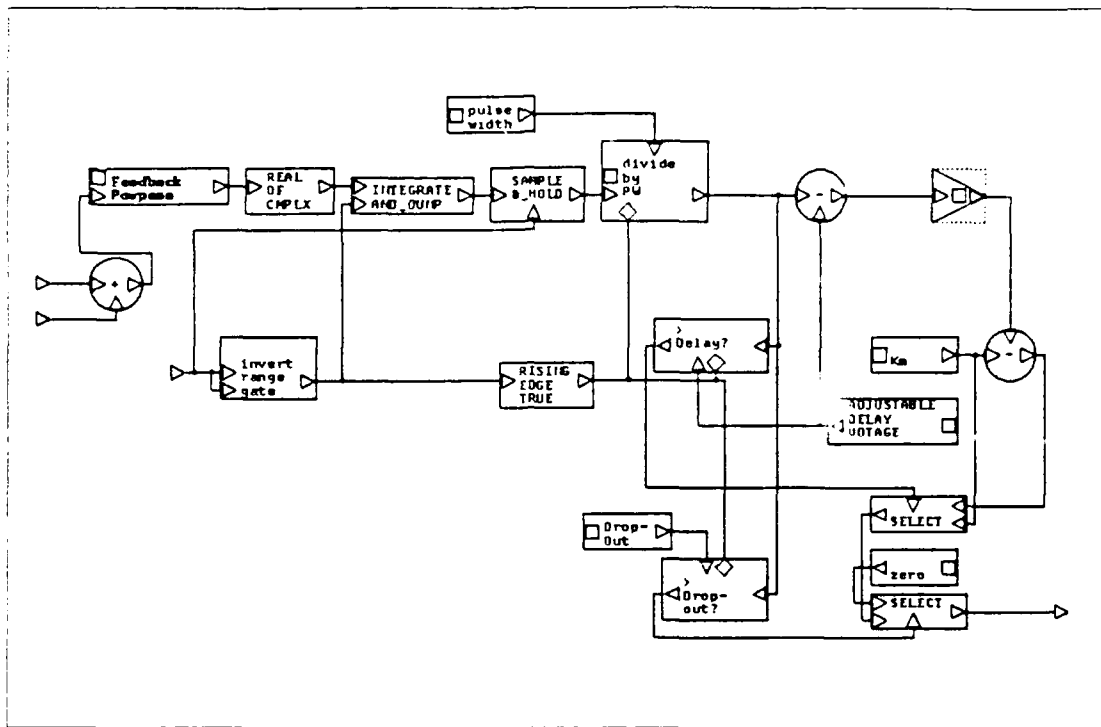


Figure 3.12. The AGC Detector Module Implemented in BOSS

were $F_2(p)$ is Leonov's notation for the frequency response of the low pass filter. This expression for the AGC voltage was included in Eq 3.2 and used to implement an AGC module in BOSS.

Assuming a corner frequency of 5 Hz, a time-scaled pulse width of 0.05 seconds and a PRI of 0.5 seconds (PRF of 2 HZ), the effective time constant of the AGC detector can be calculated using equation 2.19

$$T_{pulse} = \left(\frac{1}{5}\right) \left(\frac{0.5}{0.05}\right) = 2 \text{ seconds} \quad (3.12)$$

which equals forty pulse-widths, a value consistent with Lawson's description of IAGC [8:313].

3.3.3 *The AGC Detector Implemented in BOSS.* The final implementation of the AGC detector module is shown in Figure 3.12. The two input signals are combined and passed through a **FeedBack LPF** which is actually a **1st Order Butterworth Low-Pass Filter**. The expressions describing the AGC response were developed for a 1st order feedback filter. Since this filter is operating on the sum of the two IF filters' outputs, the impulse response (a function of a filter's order) of this filter is not critical. The feedback filter serves primarily to set the frequency response of the feedback loop. Given that the inputs to this filter are prefiltered by the IF filters, so long as the corner frequency of the feedback filter are well below those of the IF filters, the order of the filter is not critical.

The output of the feedback filter is input into a chain of modules, beginning with the **REAL OF CMPLX** and ending with the **Divide by PW** module, which sample the output of the low-pass filter (only during the range gate period) and calculate the average. This average value is compared to the output of the **Adjustable Delay Voltage** with the **>DELAY?** module to determine if the desired threshold value has been exceeded. The output is also compared to the AGC drop-out level (equal to the maximum input level, or 50dB in this case) via the **>Drop-out?** module. The delay voltage is subtracted from the output of the low pass filter (equivalent to the $U_{out} - U_d$ portion of Eq 3.11) before it is amplified by the gain module. The gain is set equal to $X \times A_f$ and the result is subtracted from the max gain value A_o (labeled K_m).

The output of the subtractor (point 'A') now corresponds with Eq 3.2. The max gain value K_m is also available as a separate result, as is a constant value of zero. The transition between these three possible outputs is controlled by the result of the **>REAL** and **>Drop-out?** modules which acts as "on/off" switches via the two **Select** modules. The output of the **AGC Detector** is the desired IF gain in dB. If the output of the Low-pass filter loop is less than the delay voltage, then the resulting control signal is set equal to K_m . If the output is *greater* than the delay voltage but

less than the drop-out level, then the control voltage is given by Eq 3.10. If the high gain has caused the output of the low-pass filter to exceed the drop-out level, then the control voltage is set equal to zero.

Hughes presents a simple formula for converting from power levels in dBm (P) to peak-to-peak voltage levels for a 50Ω receiver system.

$$e_{pp} = (0.63)10^{P/20} \quad (3.13)$$

Using this formula and the values selected for the limits of the dynamic range for this AGC design

$$\begin{aligned} e_{pp}(min) &= (0.63)10^{-70/20} \approx 200\mu\text{Volts} && \text{AGC delay voltage} \\ e_{pp}(max) &= (0.63)10^{-20/20} \approx 63\text{mV} && \text{AGC Drop-out level} \end{aligned} \quad (3.14)$$

3.3.4 The Other BOSS Modules Unique to the AGC Model. The Initialize Gain module converts the output of the AGC Detector given in dB, to a absolute gain value. This module also sets the gain equal to '1' for the very first sample period (needed to allow for an output upon which to base the first AGC calculation.) The output of the Initialize Gain module is passed through a Unit Delay module which provides one simulation period (one "dt" in BOSS notation) of time delay. This unit delay is required by BOSS in any closed loop feedback application. Since one AGC loop controls the gain of both IF channels, it isn't possible to manually set the gain values of the two channels as was done for the Log-Amp model. For a gain imbalance to exist in an actual AGC based monopulse processor, the two IF amplifiers would need to have different responses to the gain control signal from the AGC detector. The Gain Imbalance module allows the specification of an imbalance of gain between the two parallel channels by exporting a parameter "Gain Imbalance

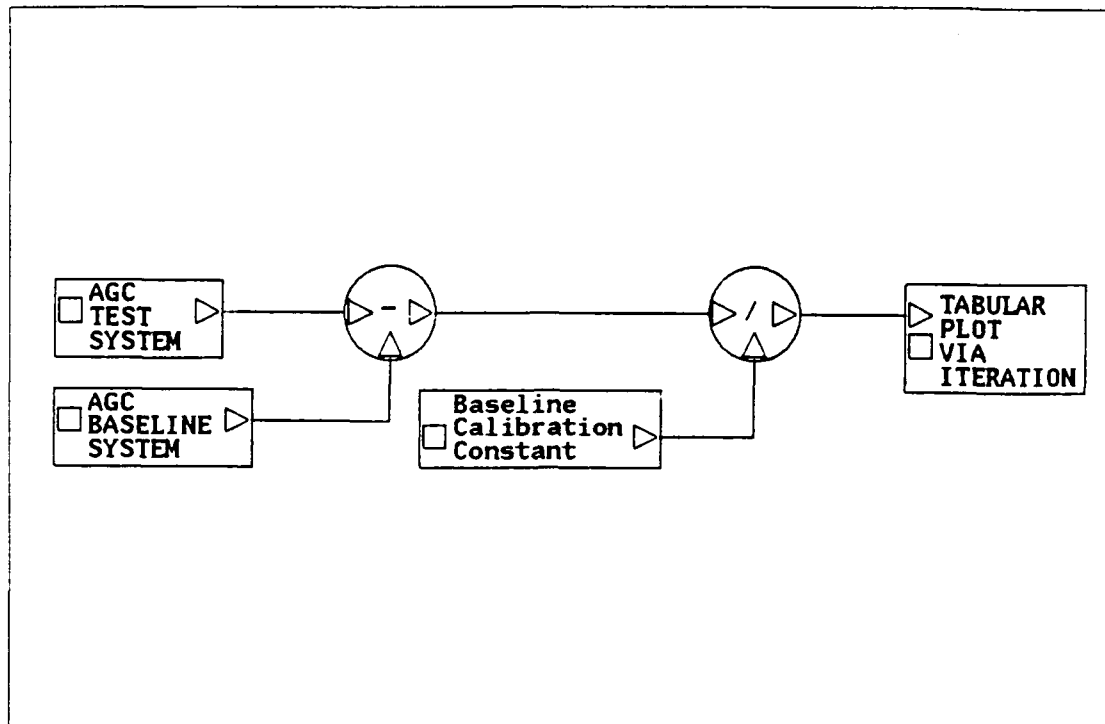


Figure 3.13. AGC-Type System Model for Calculation of Angular Errors

in %". This module increases or decreases the gain value fed to the lower channel by the specified amount to simulate an imbalanced gain response in the receiver channels. For a balanced system, the gain imbalance is set equal to zero and both IF amplifiers receive identical gain control signals.

3.3.5 AGC System Angular Error Model. Once again, to conform to the definition established in Eq 3.1, the output of a complete AGC-Type Monopulse processor model with balanced gains and frequency response was subtracted from the model under test. This gave Δ_{ratio} which was then divided by the slope of the balanced model's monopulse ratio to yield the angular error, which was plotted via the Tabular Plot via Iteration module. The blocks labeled AGC Test System and AGC Baseline System are complete AGC-Type Monopulse Processor modules as shown in Figure 3.10 with the plot accumulator removed.

Table 3.2. The Significant Parameters Used in the AGC System Simulation

Parameter	Sub-Module Used in	Set To	Exported As
SNR	Received Signal Generator	-	real
Noise On-Time	Received Signal Generator	-	seconds
Impulse Delay	Received Signal Generator	-	seconds
Pulse Rate	Received Signal Generator	-	Hz
Time of Impulse	Received Signal Generator	-	seconds
Angle Off Boresight	Received Signal Generator	-	milliradians
Gain Imbalance (in %)	Gain Imbalance	-	percentage
V1 Filter Edge Freq.	V1 Channel	20 Hz	-
V2 Filter Edge Freq.	V2 Channel	-	real
Max Gain	AGC Detector	60 dB	-
Loop Gain	AGC Detector	41 dB	-
Delay Voltage	AGC Detector	10^{-2}	-
Drop-Out Level	AGC Detector	.063	-
FeedBack Filter	AGC Detector	5Hz	-
Pattern Factor	Received Signal Generator	7.0711^{-9}	-
Calibration Constant	Signal Generator	-	real

3.3.6 *Parameters Used in the AGC Model.* The parameters which were exported to the top level of the simulation are show in table 3.2. Just as was done for the Log-Amp simulations, these parameters were changed as needed prior to each simulation run to explore the effects of system imbalances.

With the models of the two processors implemented in BOSS, simulations were run to explore the response of the models in various configurations.

IV. Results

4.1 General Simulation Parameters

4.1.1 *A Basic Assumption.* Prior to investigating the effects of any imbalances in a monopulse receiver, a basic assumption concerning the simulations must be made. It is assumed that the processor is unaware of the imbalances, and that it is operating as if no imbalances were present. The validity of this assumption is, of course, dependent upon the degree of self-testing and fault reporting that is incorporated into the receiver. For these simulations, we must assume that the imbalance conditions are not severe enough to cause the processor to declare itself inoperative. This assumption's validity will depend upon the characteristics of the specific hardware implementation of the monopulse processor one is operating against.

4.1.2 *Baseline Simulations.* A baseline (also referred to as a "balanced") simulation for both models was defined as one in which the corner frequencies as well as the gains of the two channels' low-pass filters were set equal to one another. The following conditions defined a baseline:

1. IF filters were set for 20Hz corner frequencies. Assuming a 2MHz actual IF Filter is being simulated, this represents a 10^5 down-scaling of frequency, which also implies a multiplication of time by the same factor.
2. 20Hz filters correspond to a .05 second pulse width for the signal pulse if it is assumed that a matched filter is approximated by a filter with a bandwidth equal to the inverse of the pulse width.
3. The simulation sampling interval was chosen to be 0.001 seconds. Digital simulation theory tells us that this corresponds to a maximum simulation frequency of $1/0.001 = 1000\text{Hz}$. Additionally, Nyquist's criterion gives a maximum unambiguous simulation frequency of 500Hz which is well above the 20Hz corners of the modeled IF Filters.

4. To reduce the effect of random errors, and to improve the detection range, most monopulse processors non-coherently integrate (average) the returns from a number of pulses. Ten video pulses were averaged in the simulations.
5. To simulate a null-tracking radar, the target was assumed to be near the bore-sight of the antenna. BOSS allows for a maximum of nine iterations of a single parameter during a simulation. The parameter "Angle off Boresight" was iterated from $-.004$ radians to $+.004$ radians in nine steps of $.001$ radian each.

4.2 *Determination of Calibration Constant.*

The first set of simulations were performed to establish the slope of basic monopulse ratio of the Log-Amp and AGC Systems under balanced (ideal) conditions. This slope was used as the calibration constant in all subsequent simulations which used the "Angular Error" models. The endpoints of Figures 4.1 and 4.2 were examined using BOSS's capability to display the x,y value of any point on a graph by clicking the mouse pointer over the point. The slopes were determined by dividing the ordinate value of the far right endpoint by 0.004.

$$\begin{aligned} \text{Log-Amp Calibration Constant} &= \frac{1.0676 \times 10^{-6}}{.004} = 2.669 \times 10^{-4} \\ \text{AGC System Calibration Constant} &= \frac{.00263}{.004} = 0.6575 \end{aligned}$$

4.3 *Simulations to Establish the Effect of the Time of the Impulsive Jamming*

Since the simulations will all be based upon the idea of averaging the monopulse result over 10 received signal pulses, it was desired to establish the effect of applying the impulse at different points in this sequence of ten pulses. For this purpose, simulations were run with an arbitrarily chosen impulse delay of 0.02 seconds following the leading edge of either the first, fourth, or tenth pulse in the train of received pulses with the resultant errors in indicated target position recorded.

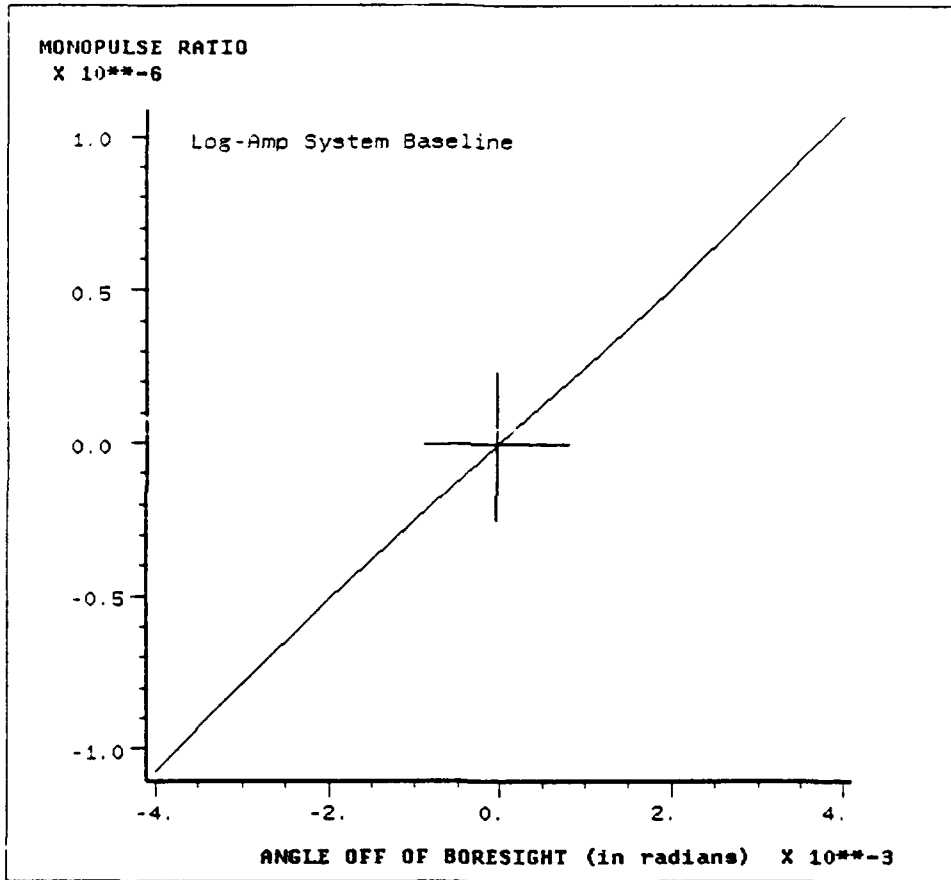


Figure 4.1. Baseline Monopulse Ratio Plot for Log-Amp System

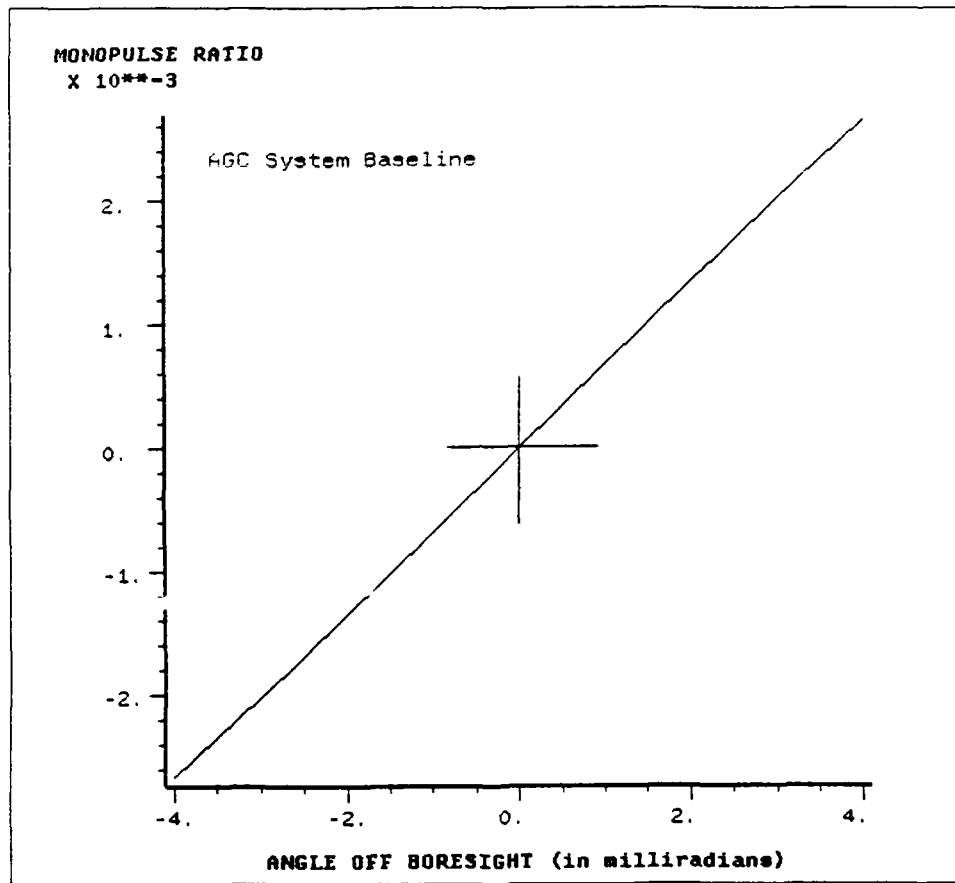


Figure 4.2. Baseline Monopulse Ratio Plot for AGC System

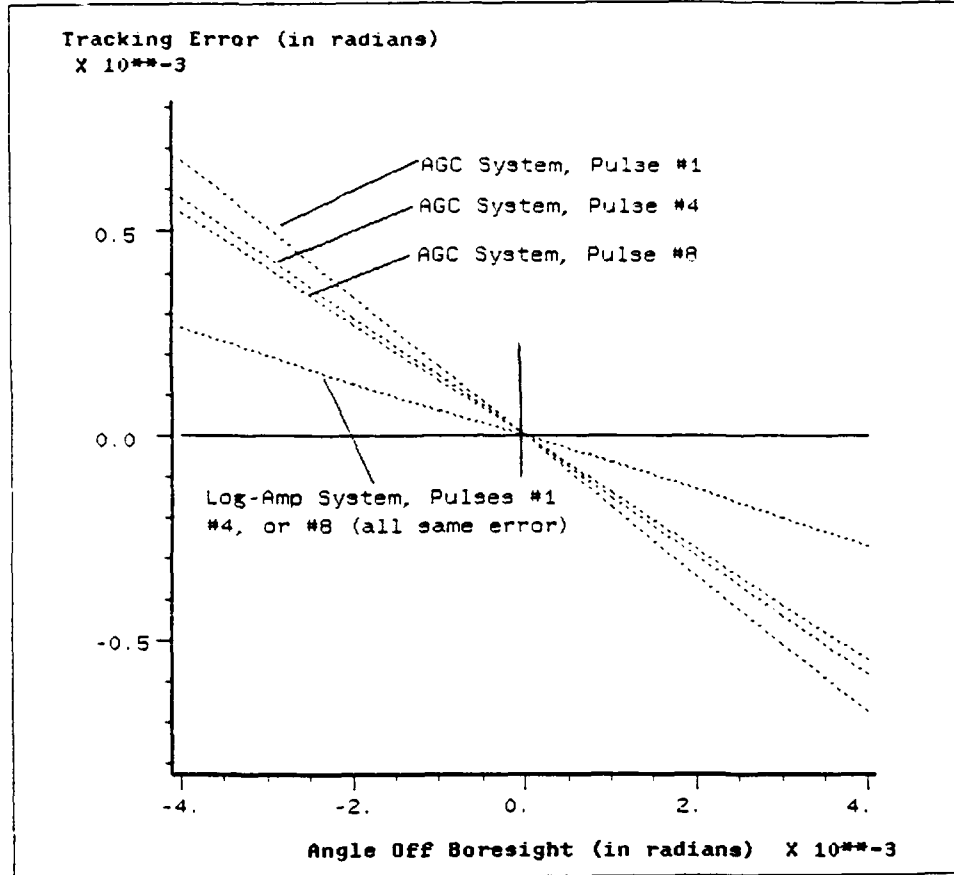


Figure 4.3. Angular Errors Induced in Both Log-AMP and AGC-Type Monopulse Systems for an Impulse Applied During Received Pulse #1, #4, or #8 in a Train of 10 Pulses under Balanced Conditions

All of these simulations were run with the gains and frequency responses balanced with only the arrival time of the impulse changing between simulations.

The results of these simulations are presented in Figure 4.3.

The Log-Amp provides nearly instantaneous normalization of the signal, so it would be expected to demonstrate the same response for an impulse applied at any point in the signal train. The AGC system however, should experience a reduction in gain following the impulse that should persist for several pulses even after the impulse is removed as the AGC recovers to its normal gain value. For this reason,

the AGC system will be most sensitive to impulses applied early into the train of pulses, because this condition will effect the measurement made on more pulses than if the impulse is delayed farther into the train of ten pulses. This is illustrated by the actual data plots of Figure 4.3.

Since the AGC system's errors were largest for an impulse applied during the first pulse and the Log-Amp system was insensitive to the timing of the the impulse, to obtain "worst case" results all subsequent simulations which indicate that an impulse is used will have the impulse applied during the first received pulse.

4.4 Basic Noise Influence Tests

This research was not intended to include an in-depth analysis of the effects of system noise upon the angular errors induced. However, a few basic simulations were run to demonstrate the effect of additive white gaussian noise (AWGN) upon the angular errors. The Log-Amp Angular Error simulation was run for four simulations:

1. Balanced system, no noise with no impulse.
2. Balanced system, 20db SNR with no impulse.
3. Balanced system, no noise with an impulse applied during the first pulse.
4. Balanced system, 20db SNR with an impulse applied during the first pulse.

The results are presented in Figure 4.4 and one can see that the noise basically caused the error to vary about the line representing the error observed in the absence of the noise. The maximum amount of the error attributable to the noise alone for an amplitude comparison monopulse system is predicted by Leonov [9:202] as

$$\sigma_{\theta} = \frac{(0.5)\theta_{0.5}}{\sqrt{\frac{S}{N}n}} \quad (4.1)$$

where n is the number of pulses averaged during detection. Using a 20db SNR and

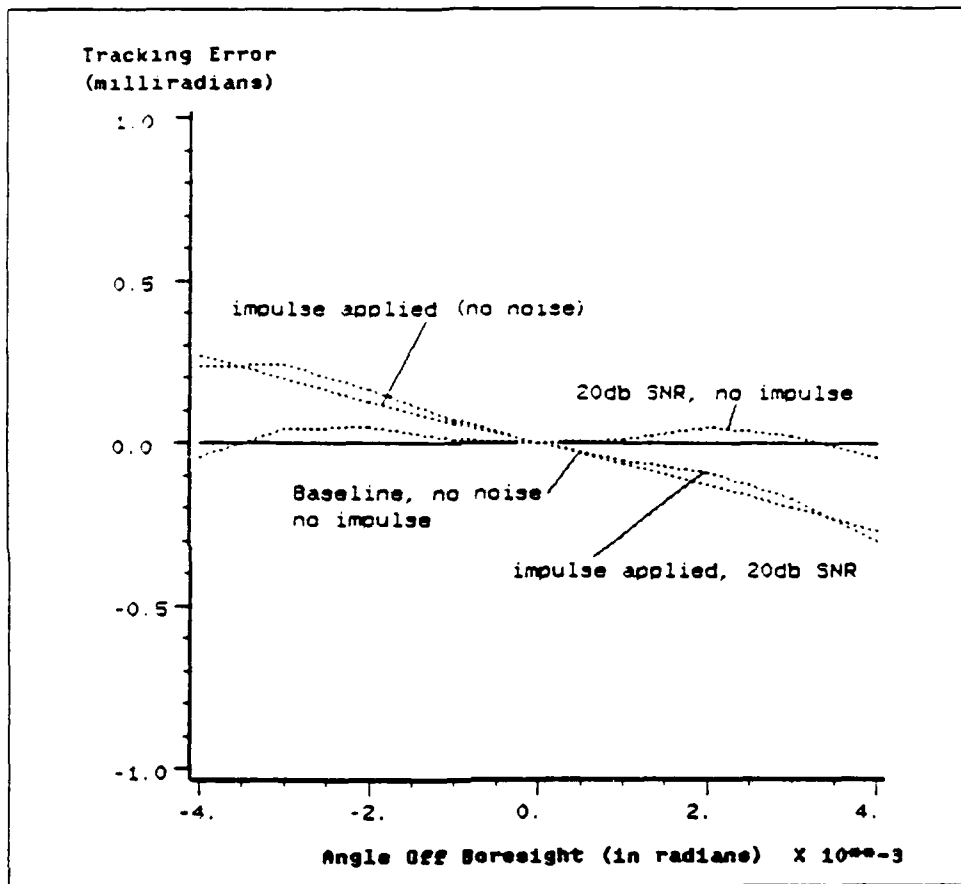


Figure 4.4. Angular Errors in a Balanced, Log-Amp System due to AWGN in Conjunction With an Impulse

10 pulse integration with a reference beamwidth of 20 milliradians, the possible error is

$$\sigma_{\theta} = \frac{(0.5)20}{\sqrt{10010}} = 0.316 \text{ milliradians} \quad (1.2)$$

and we see that the plotted value is well within this limit. A possible explanation as to why the limit wasn't approached in these simulations is that BOSS uses a "seed" value in a random number generator to generate the random noise. Since each plot in Figure 4.4 is the result of nine iterations, the random number generator had only nine opportunities to generate a number that was approaching the maximum variance value specified during the simulation. Perhaps if BOSS would allow more than nine iterations, the noise plots would have exhibited greater deviation about the mean.

No other simulations with noise included were conducted.

4.5 *Simulation Matrices*

Each simulation was named to indicate the conditions under which it was run. The first two letters in the name "NN..." indicate that no noise was injected into the received signal. The second two characters in the name specify whether or not there was an impulse present during the first pulse of the pulse train. If no impulse was present, "... NI- ..." was used, while "... I2- ..." indicates that an impulse was injected in the received signal (the 2 indicates that the impulse was delayed 0.02 seconds from the leading edge of the first pulse). The final characters specify the type and degree (in percent) of imbalance that was present between the two channels of the processor under test. "BL" indicates a baseline simulation with no imbalances, while a "G" is used for gain imbalances and a "F" represented an imbalance in the corner frequencies of the IF filters. Thus, "NNI2-G5(+)" would be read as "No Noise, Impulse used - Gain imbalance of +5%". The v1 (or upper) receiver channel is assumed to remain fixed at the design frequency (normalized to 20Hz in the model) and gain and any references to positive or negative frequency or

Table 4.1. Gain Imbalance Runs for Both LOG-AMP and AGC-Type System

Simulation	Gain Imbalance		Impulse	
	0%	+5%	Yes	No
NNNI-BL	X			X
NNI2-BL	X		X	
NNNI-G5(+)		X		X
NNI2-G5(+)		X	X	

Table 4.2. Frequency Imbalance Simulations for AGC-Type System

Simulation	Frequency Imbalance						Impulse	
	-15%	-5%	0%	+5%	+10%	+15%	Yes	No
NNNI-F15(-)	X							X
NNI2-F15(-)	X						X	
NNNI-F5(-)		X						X
NNI2-F5(-)		X					X	
NNNI-BL			X					X
NNI2-BL			X				X	
NNNI-F5(+)				X				X
NNI2-F5(+)				X			X	
NNNI-F10(+)					X			X
NNI2-F10(+)					X		X	
NNNI-F15(+)						X		X
NNI2-F15(+)						X	X	

gain imbalances are with reference to this channel.

4.5.1 Simulations with Gain Imbalances. To explore the effect of a gain imbalance between the two parallel receiver channels, both the Log-Amp and AGC-Type models were run with the conditions specified in Table 4.1.

4.5.2 Simulations with Frequency Imbalances. The effect of a frequency imbalance between the two parallel receiver channels for both Log-Amp and AGC-Type models were examined using the conditions set forth in Table 4.2 and Table 4.3.

Table 4.3. Frequency Imbalance Simulations for LOG-AMP Type System

Simulation	Frequency Imbalance					Impulse	
	-15%	-5%	0%	+5%	+15%	Yes	No
NNNI-F15(-)	X						X
NNI2-F15(-)	X					X	
NNNI-F5(-)		X					X
NNI2-F5(-)		X				X	
NNNI-BL			X				X
NNI2-BL			X			X	
NNNI-F5(+)				X			X
NNI2-F5(+)				X		X	
NNNI-F15(+)					X		X
NNI2-F15(+)					X	X	

The "+10% Frequency Imbalance" runs for the AGC-Type system were added after the results of the other conditions were examined to more accurately define the behavior of that system for larger degrees of frequency imbalance.

4.6 Gain Imbalance Results

The results of the gain imbalance runs for the Log-Amp type system are presented in Figure 4.5. An impulse alone, with no system imbalances, can cause a small error as the target moves away from the boresight. This is due to the initial conditions on the IF filters which vary with the changing levels of the v_1 and v_2 signals (which are a function of target location.)

The IF filters were modeled as ideal (and therefore linear) low-pass filters. One would expect their final impulse response to be the sum of the pure (zero voltage initial condition) impulse response plus the value of their output due to the initial condition imposed by the v_1 and v_2 signals. This is indeed the case, but the non-linear amplification of the logarithmic amplifier model caused the amplified impulse response to differ by an amount that was not linearly related to the magnitude of

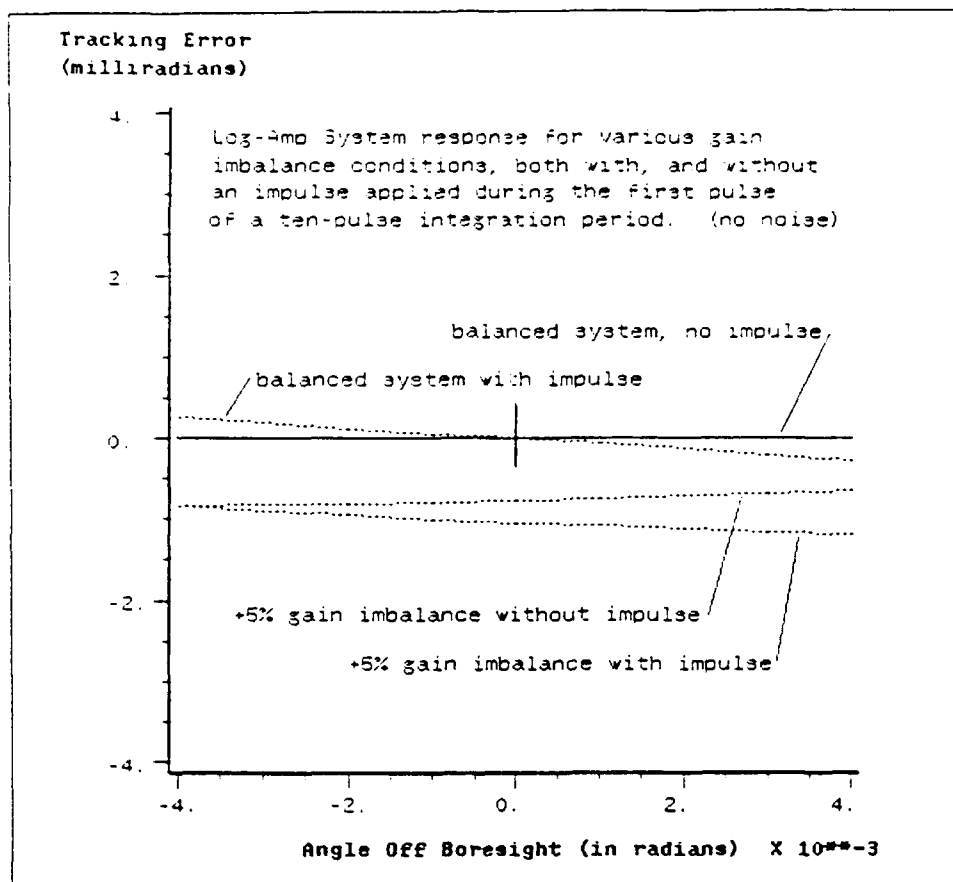


Figure 4.5. Angular Errors in Log-Amp System Output for a 5% Gain Imbalance (with and without an impulse applied)

the filters' outputs prior to the impulse.

This non-linear amplification caused the monopulse ratio to be altered (resulting in an error in the indicated angle) during the processing of the pulse with the impulse applied, and this error was then averaged with the results during the nine other pulses which were processed without an impulse present. The introduction of a gain imbalance adds a bias to the previously discussed results. The bias is nearly constant, with the small slope due, once again, to the non-linear amplification of the logarithmic amplifier.

Considering that even the most accurate monopulse systems can maintain at best approximately 0.1 milliradian accuracy, the additional error introduced to a balanced Log-Amp processor by hitting it with an impulse is probably not large enough to serve as an effective countermeasure [1:247]. Similar results are seen in Figure 4.6 for the AGC based processor. The error curves exhibit the same basic characteristics as those for the Log-Amp processor. In this case, it was the non-linear characteristics of the AGC circuitry which introduced the slope in the curves.

Since the modeled AGC circuit's time constant was several times longer than that of the IF filters, the AGC required several pulses to recover following the application of a single impulse. Consequently, the magnitude of the induced error was understandably larger for this processor than for that of the Log-Amp processor. More of the processed pulses are affected by the impulse for the AGC based processor.

The magnitude of the errors in this case may be significant enough to cause a noticeable decrease in the accuracy of even a balanced tracking radar if impulses can be applied early in the train of integrated pulses.

4.7 Frequency Imbalance Results

A change in the corner frequency of the models' low-pass filters corresponded to an equivalent change in the bandwidth of the modeled IF filters. As the corner

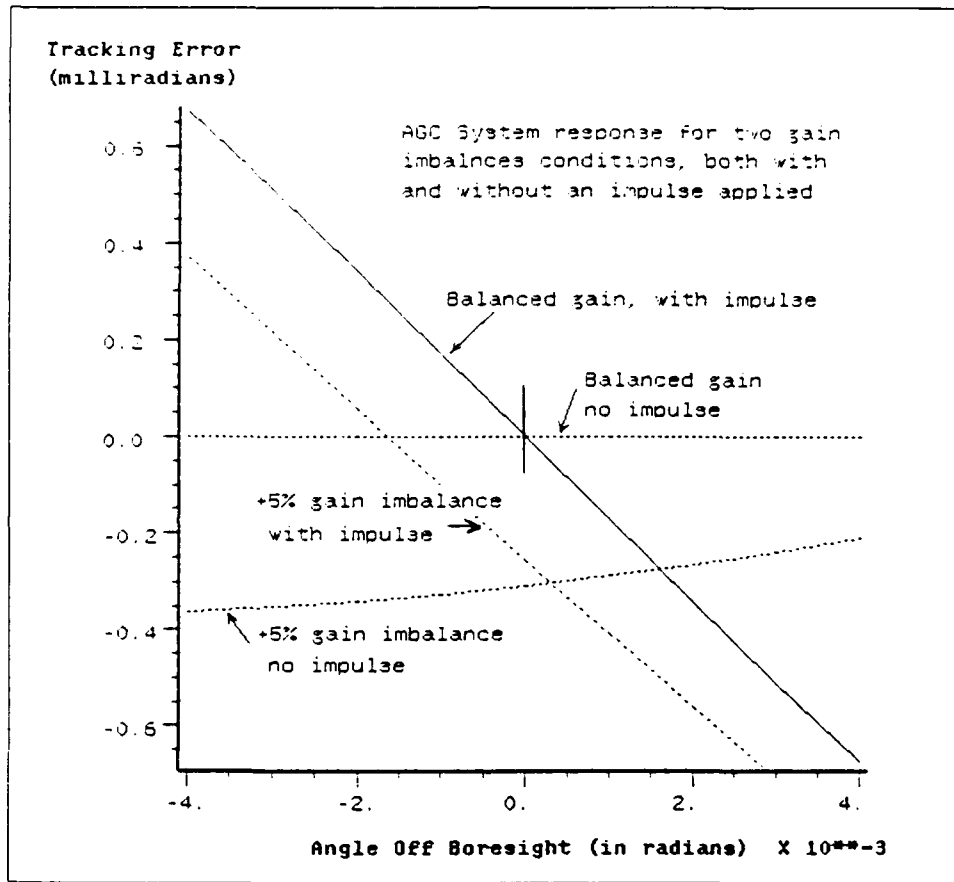


Figure 4.6. Angular Errors in an AGC-Type System for 5% Gain Imbalance (with and without an impulse applied)

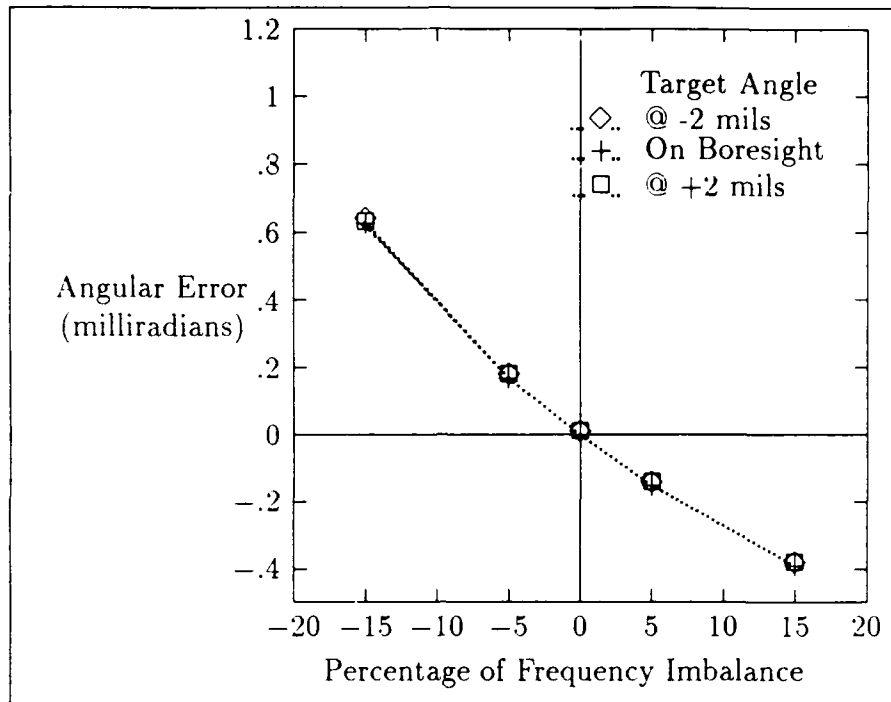


Figure 4.7. Angular Errors Induced in Log-Amp System as a Function of Frequency Imbalance, *No Impulse Applied*

frequency of the low-pass filter was changed, the filter's impulse response changed also. Generally, a higher corner frequency results in an impulse response which reaches its peak magnitude (and then crosses through and oscillates about zero) earlier than a similar filter with a lower corner frequency. Also, since the receiver was assumed to be matched to the received pulse width, any deviation from the designed operating frequency affected that filter's response to the incoming pulse. One could therefore expect that if the two parallel IF filters had non-identical frequency characteristics, then some error will be introduced into the final monopulse result both with and without an impulse accompanying the received pulse, and data reflected this tendency.

4.7.1 Log-Amp Frequency Imbalance Results. The errors introduced in a Log-Amp monopulse processor due to frequency imbalances alone are presented in Fig-

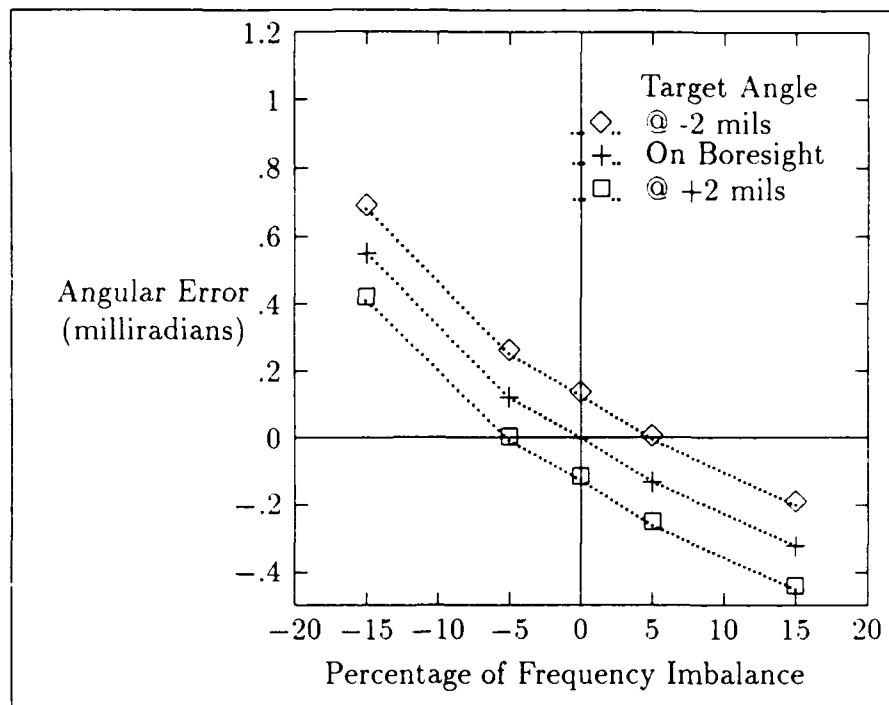


Figure 4.8. Angular Errors Induced in Log-Amp System as a Function of Frequency Imbalance, *With Impulse Applied*

ure 4.7. The errors are nearly a linear function of the degree of frequency imbalance and are not a function of the target's angle for targets near the boresight. As we see in Figure 4.8, the introduction of an impulse added a small bias to the results obtained without an impulse, and the bias was a function of the target's angle from the antenna's boresight.

4.7.2 AGC Frequency Imbalance Results. The impact of frequency imbalances for the AGC based processor in the absence of an impulse are shown in Figure 4.9. As in the Log-Amp processor tests, we see that the error was nearly a linear function of the frequency imbalance and was not strongly dependent upon the target's location. The AGC based monopulse processor's errors in the presence of both a frequency imbalance and a jamming impulse are presented in Figure 4.10. This plot demonstrates the similarity between this system's response and the response of

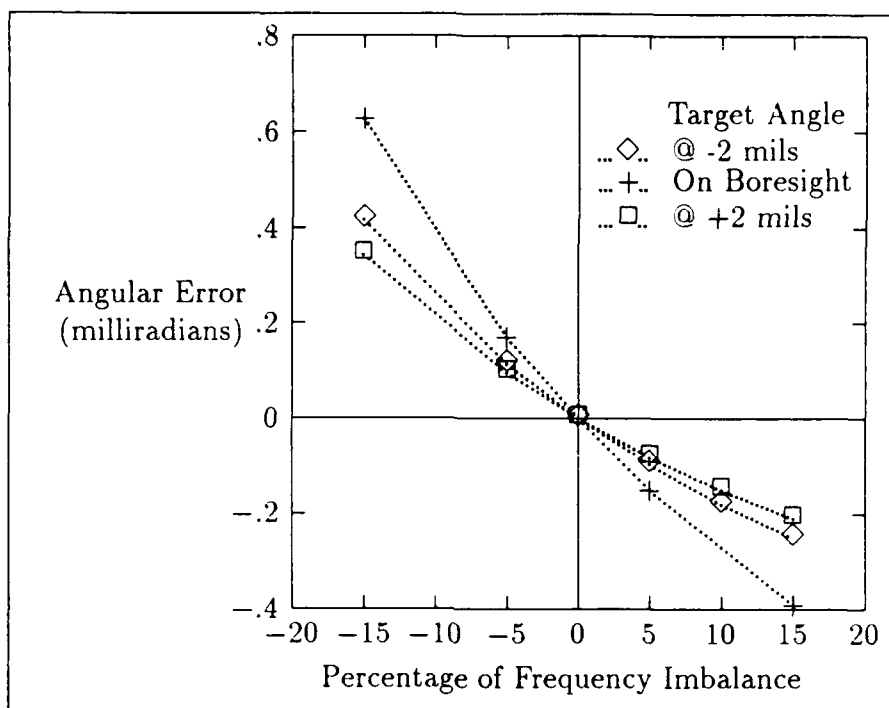


Figure 4.9. Angular Errors Induced in AGC Based System as a Function of Frequency Imbalance, *No Impulse Applied*

Log-Amp based processor for *negative* frequency imbalances. The impulse caused a nearly constant bias in the amount of error, as a function of target angle, until the frequency imbalance approaches +5%. For imbalances greater than this, the errors converged to nearly identical values regardless of the target's position, and their magnitudes increased significantly.

This significant increase in the magnitude of the error was due to two factors. First, for frequency imbalances above +5%, the increased bandwidth of the v_2 channel caused the impulse response of the IF filter to begin to ring through zero within the range gated time interval. This caused a sign reversal of the v_2 value. Since the subtractor calculates $(v_1 - v_2)$, as v_2 goes negative, the subtractor functions as an adder. Secondly, this occurred before the AGC detector could lower the gain of the two channels, and the error is magnified by the large gain values established by the

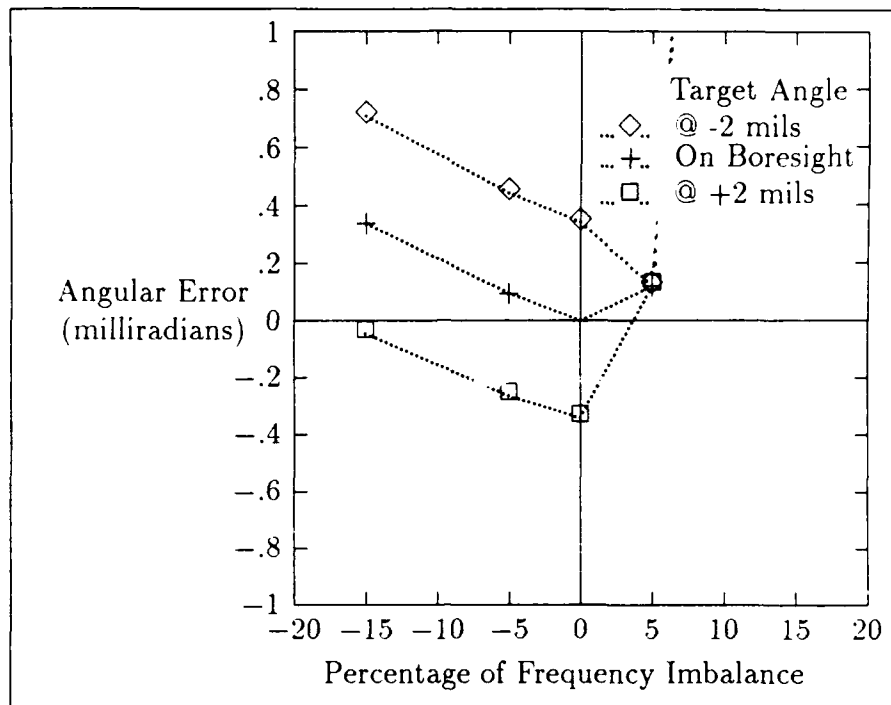


Figure 4.10. Angular Errors Induced in AGC Based System as a Function of Frequency Imbalance, *With Impulse Applied*

previous pulse's signal level. These higher frequency imbalance conditions did not cause excessive errors in the Log-Amp system since the IF filter's output was normalized almost instantaneously by the logarithmic amplifier. Figure 4.11 presents the same data as that of Figure 4.10, but with the increase in the vertical axis scale, we see the true magnitude of the errors induced in an AGC based processor with positive frequency imbalances when an impulse is applied. The errors may appear suspect to the processor as they represent a target that is more than *ten beamwidths* away from where the tracker originally thought the target was!

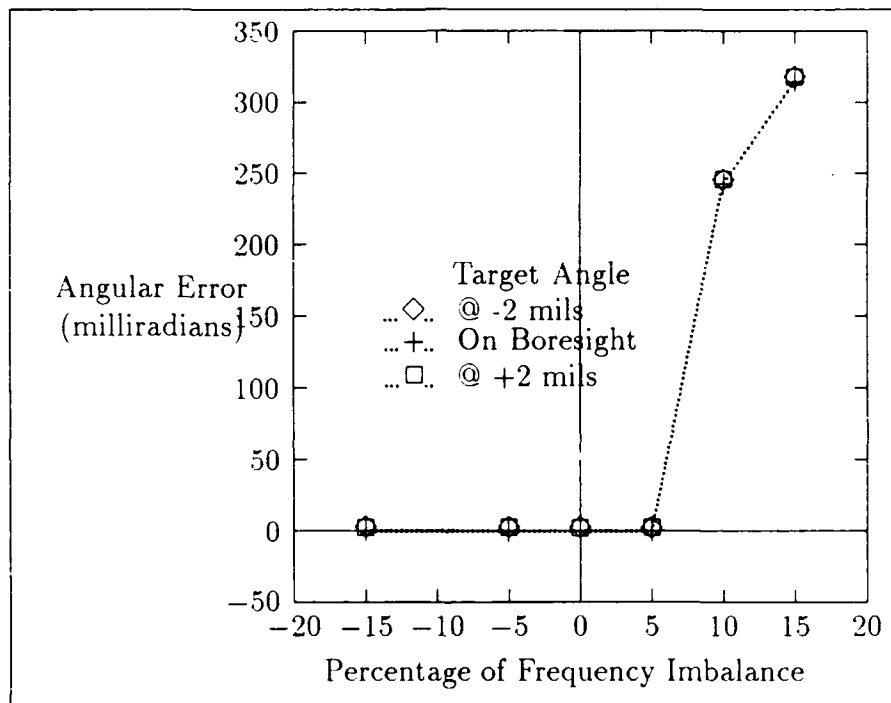


Figure 4.11. Increase in Magnitude of Angular Errors Induced in AGC Based System as Frequency Imbalance Becomes Increasingly Positive. *With Impulse Applied*

V. *Conclusions and Recommendations*

5.1 *Conclusions*

This thesis has presented BOSS models for both a Log-Amp and AGC-based amplitude comparison, monopulse processor. The effects of both gain imbalances and frequency imbalances between the two parallel processing channels were explored. The accuracy of these imbalanced systems, both with and without an impulsive jamming signal present, was established.

5.1.1 Impact of Imbalanced Systems Without Impulsive Jamming. The analysis demonstrated that without an impulse applied, both systems exhibited a small amount of angular measurement error whenever there was an imbalance between the two channels in the receiver. For gain imbalances, the error manifested itself as a nearly constant bias at all target azimuths. The amount of the error constant error was a function of the amount of gain imbalance and was generally on the order of the expected accuracy of a balanced system and in most applications would probably not be significant enough to prevent the radar from accomplishing its assigned mission.

The errors due to frequency imbalances for either type of system, in the absence of an impulsive signal, were largely a function of the degree of frequency imbalance. The errors were relatively independent of the target's position with respect to the tracking antenna's boresight. As was the case for gain imbalances without an impulse, these errors were approximately equal to the anticipated accuracy of a balanced monopulse receiver. The errors would induce an additional degree of uncertainty concerning the target's true location. However, it required a frequency imbalance of more than $\pm 15\%$ before the angular errors approached 1/2 milliradian in magnitude, indicating that these errors alone would not induce an inordinate amount of error in the receiver.

The effects of gain imbalances in monopulse receivers is well known, and several design methods are utilized to minimize the effects this type of imbalance causes. These methods include such things as switching (or commutating) the inputs to the two channels for every pulse received and thereby averaging the error toward zero, and the use of pilot pulses to adjust the variable gain amplifiers to maintain a balanced condition. Such techniques were not incorporated in the simple models developed for this thesis, and the basic errors presented are therefore always a "worst case" value from the tracking radar's point of view. These techniques should also reduce the impact of frequency imbalances between the receiver channels.

5.1.2 Errors Introduced as a Result of an Impulsive Jamming Signal. With the introduction of a single impulsive jamming signal at the beginning of an integration period of multiple pulses, it was possible to introduce angular errors in even a balanced monopulse processor. In a balanced processor, the errors induced by the impulsive signal were rather small, on the order of the expected overall accuracy of the systems, and probably not significant enough to serve as an effective countermeasure.

For systems which had an imbalance in the gains of the two channels of the processor, the impulse added a small amount of error beyond the error due to the gain imbalance alone. The AGC-based system was more susceptible to impulse than was the Log-Amp processor.

With frequency imbalances present in the receiver, the differences between the Log-Amp system and the AGC-based monopulse processors became more evident. The Log-Amp system maintained its nearly linear relationship between the degree of frequency imbalance and angular errors for imbalances from -15% to +15% but a small bias (as a function of the target's angle) was introduced by the impulsive signal.

For the AGC-based processor, the response to the impulsive signal as a function

of frequency imbalance similar to the Lo-Amp up until the frequency imbalance began to exceed +5%. From that point on, the induced angular error ceased to be a function of target angle and increased dramatically as the frequency imbalance became more increased. In terms of inducing an angular measurement error, *an impulsive jammer would clearly be most effective against a frequency imbalanced AGC-based processor with the imbalance greater than +5%.*

5.1.3 Timing of Impulse and Effect of Noise Upon Induced Errors. The presence of AWGN did not appear to influence the basic errors in the angular measurement other than to distribute the error about the value that would have existed without noise. The Log-Amp based processor, with its nearly instantaneous normalization was insensitive to the position of the pulse within the received pulse train. To introduce errors in an AGC-based processor, the best time to apply a single impulsive signal is as early in the integration period as possible. This timing takes maximum advantage of the period of reduced sensitivity in the receiver which exists for several pulse periods following the reception of an impulsive jamming signal.

5.1.4 Interpretation of the Sign of the Error. The importance of the sign of the angular errors presented here should also be considered. If the target is located to the right of the antenna's boresight (the indicated is + by the convention used in this thesis) and the angular error induced is also (+), then the error might cause the antenna to overshoot the target. On the other hand, if the target's true angle is (+) and the error induced is (-), then the antenna would fail to move enough and might lag the target's movement.

In either case, one must consider the effects possible if the jamming can be sustained in a repeatable fashion, perhaps coordinated with the monopulse radar's transmitting scheme. For this situation, dependent upon the degree of imbalance in the processor, the errors could cause the radar to track in the wrong direction relative to the target's movement. This error in direction could excite instability

in the tracking servo-mechanisms and therefore eventually cause a break-lock. The errors could also simply cause a lag in the indicated target angle. The obvious difficulties from the jammer's point of view are numerous. The jammer would require a knowledge of the degree of the radar's imbalance as well as location of the target relative to the radar's boresight in order to cause a predictable and repeatable error in the tracking radar.

5.2 Recommendations

Suggestions for further research on this subject would include the following:

1. Continuation of this effort to include *phase comparison* monopulse processors.
2. Investigation of effects of differing values of AGC response time.
3. Inclusion of a typical servo mechanism used to drive a tracking antenna in the model to investigate the optimum rate to apply jamming pulses against a close loop tracking system.
4. Determine the sensitivity of the errors induced to the basic monopulse ratio slope of different processors.

Appendix A. AGC Reaction to Impulsive Signal

This appendix will present plots which demonstrate the performance of the AGC Detector for both a pure received signal pulse train and for a pulse train containing an impulse. Figure A.1 shows the output of the IF amp (pulse rate = 2Hz) with

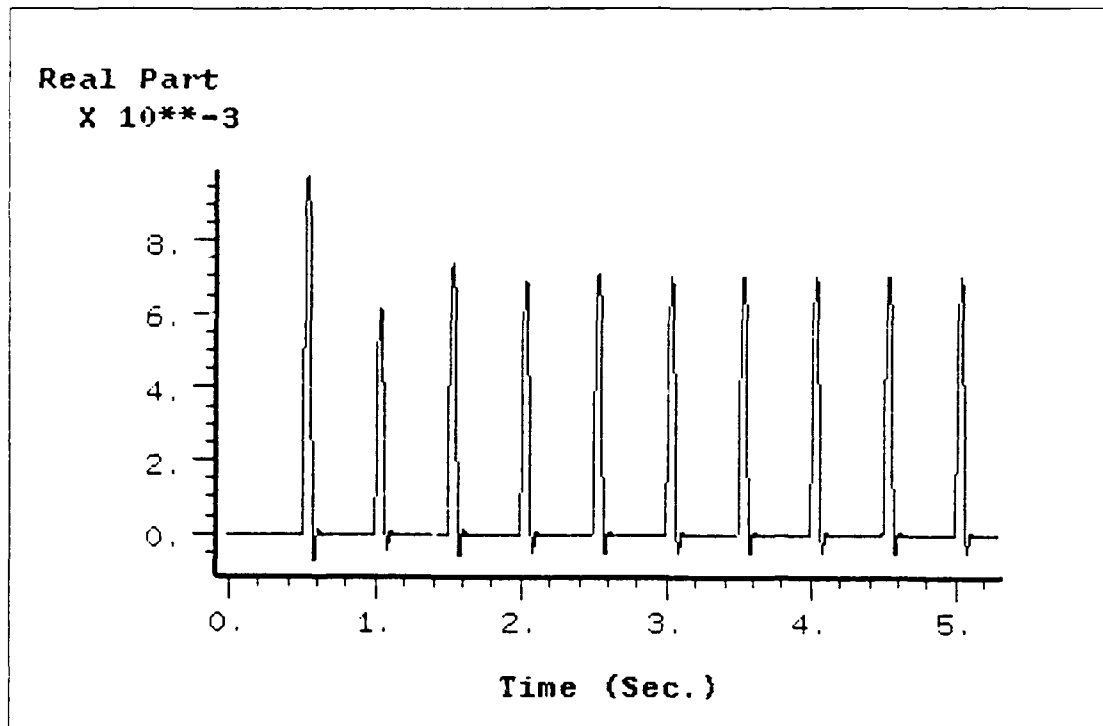


Figure A.1. IF Filter Output Showing Effect of AGC Gain

the AGC detector operating within its normal dynamic range. Figure A.2 shows the corresponding AGC gain control voltage which produced the IF plot shown in Figure A.1. The AGC gain control voltage is, for this model, the desired gain in db of the IF amp. After an impulse is applied (at $t=2$ secs), we see in Figure A.3 that the gain is initially so high that the impulse response of the IF amp is amplified greatly. This causes the AGC detector to reduce the gain (see Figure A.4) for the

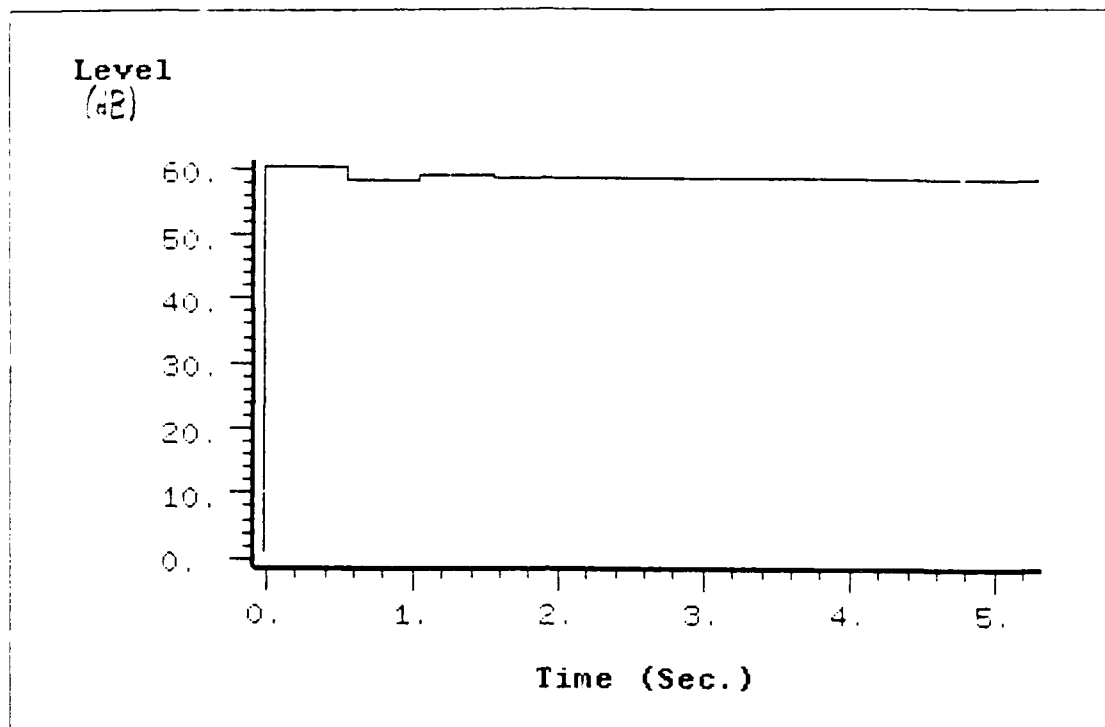


Figure A.2. AGC Gain Control Voltage, Normal Operation

following few pulses, and therefore disturbs the IF response for several pulses even after the impulse has passed.

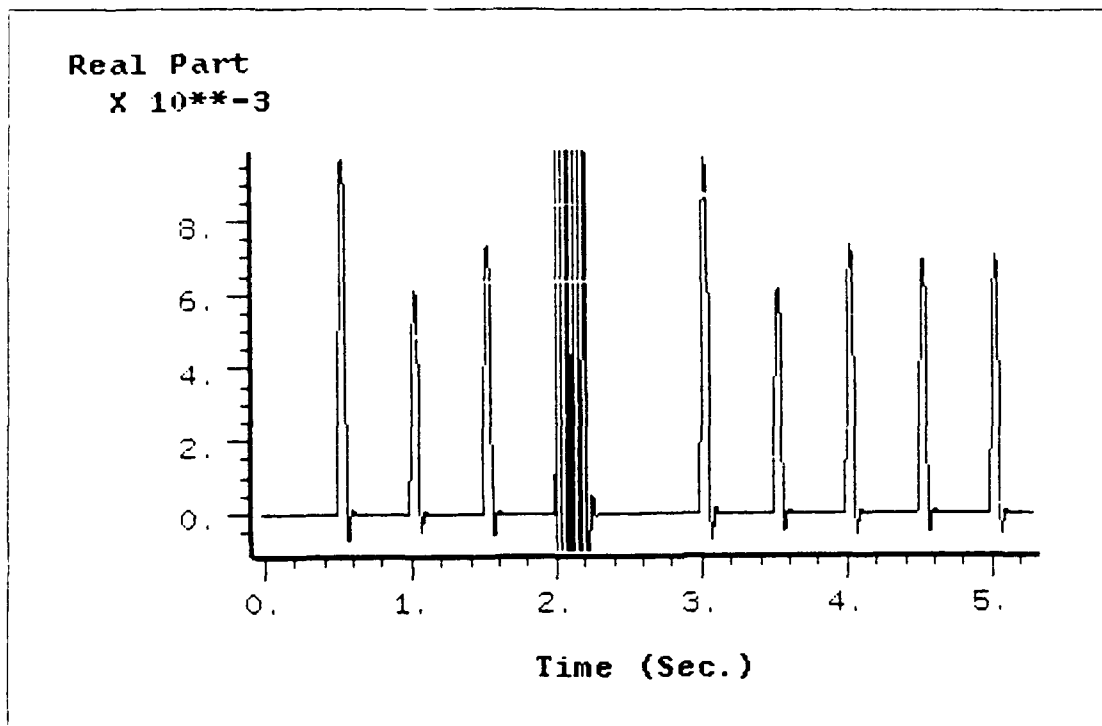


Figure A.3. IF filter Output with Impulse Applied at T=2.0 seconds

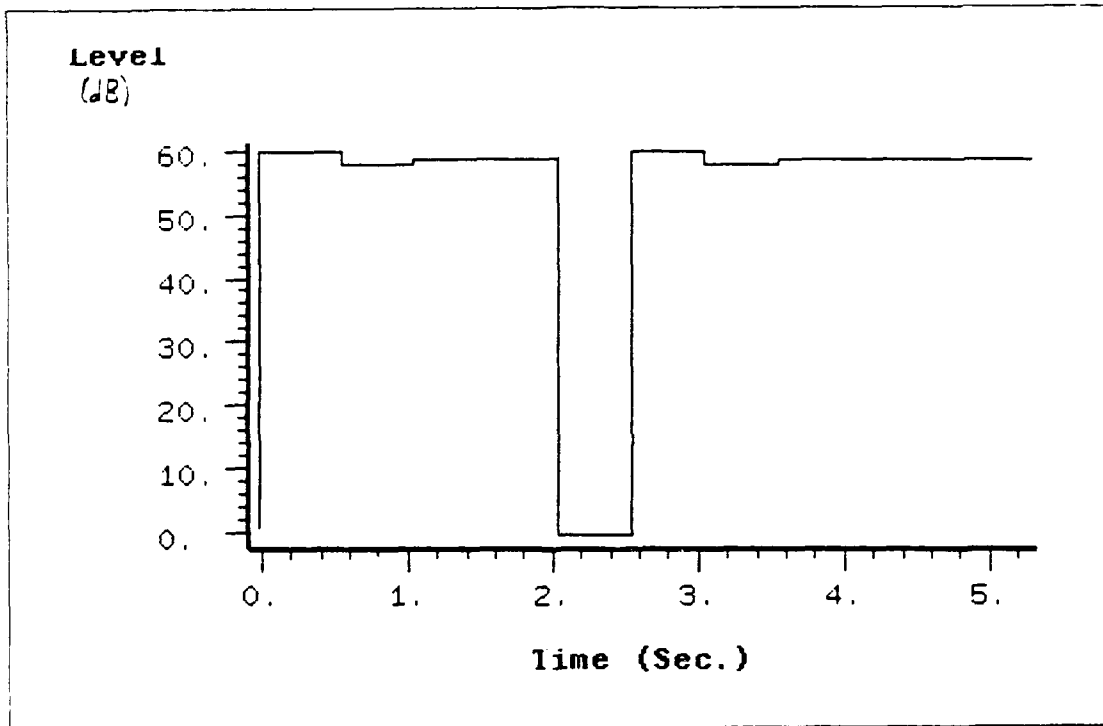


Figure A.4. Gain Control Signal Showing Impact of the Impulse for Several Pulse Periods

Bibliography

1. Barton, D. K. "Future of Pulse Radars for Missile and Space Range Instrumentation." In Barton, David K., editor, *Radars*, Volume 1, Dedham, MA: Artech House, Inc., 1974.
2. Comdisco Corporation, Lawrence, KA. *BOSS (Block-Oriented Software Simulator) User's Manual (Boss version; Comdisco V2.0 Edition)*, 1986.
3. Davis, Steve. Telephone Conversation. Power Spectrum Incorporated. San Francisco, CA, 27 March 1989.
4. Hughes, Richard Smith. *Analog Automatic Control Loops in Radar and ECM*. Norwood, MA: Artech House, 1988.
5. I. Stokes and D. K. Barton. "Guided Missile Instrumentation Radar." In Barton, David K., editor, *Radars*, Volume 1, Dedham, MA: Artech House, Inc., 1974.
6. Kirkpatrick, G. M. "Final Engineering Report on Angular Accuracy Improvement." In Barton, David K., editor, *Radars*, Volume 1, Dedham, MA: Artech House, Inc., 1974.
7. Kraus, John D. *Electromagnetics* (third Edition). New York, NY: McGraw-Hill Book Company, 1984.
8. Lawson, James L. and George E. Uhlenbeck. *Threshold Signals*. New York, NY: McGraw-Hill Book Company, 1950.
9. Leonov, A. I. and K. I. Fomichev. *Monopulse Radar*. Norwood, MA: Artech House, 1970.
10. Shanmugan, K. Sam and others. "Block-Oriented Software Simulator (BOSS)." In *1986 IEEE Military Communications Conference*, pages 36.1.1-36.1.10. October 1986.
11. Sherman, Samuel M. *Monopulse Principles and Techniques*. Norwood, MA: Artech House, 1984.
12. Skolnik, Merrill I. *Introduction to Radar Systems*. New York, NY: McGraw-Hill Book Company, 1980.
13. Tackett, Dennis L. *On the Impulse Response of Monopulse Radars*. MS thesis, AFIT/GE/ENG/88D-52, Air Force Institute of Technology, School of Engineering, 1988.

Vita

Captain Jeffrey K. Long

[REDACTED] enlisted the following year in the United States Air Force. He served as an Avionics Electronics Technician while stationed at Carswell AFB, Texas until 1981. He was then accepted into the Airman Education and Commissioning Program and attended Brigham Young University from 1981 until 1985. He received his Bachelor of Science Degree in Electrical Engineering in May 1985. Following his graduation he attended Officer Training School, Lackland Air Force Base, Texas and was commissioned an officer in the United States Air Force on 29 July, 1985. He was then assigned to the 31st Test and Evaluation Squadron, Strategic Air Command, at Edwards Air Force Base, California. For the next 3 years he performed operational test and evaluation of the Offensive Radar System on the B-1B Bomber until he reported to the School of Engineering, Air Force Institute of Technology, in May of 1988. [REDACTED]

[REDACTED]

[REDACTED]

[REDACTED]

REPORT DOCUMENTATION PAGE

1a. REPORT SECURITY CLASSIFICATION UNCLASSIFIED		1b. RESTRICTIVE MARKINGS		
2a. SECURITY CLASSIFICATION AUTHORITY		3. DISTRIBUTION / AVAILABILITY OF REPORT Approved for public release; distribution unlimited		
2b. DECLASSIFICATION / DOWNGRADING SCHEDULE				
4. PERFORMING ORGANIZATION REPORT NUMBER(S) AFIT/GE/ENG/89D-26		5. MONITORING ORGANIZATION REPORT NUMBER(S)		
6a. NAME OF PERFORMING ORGANIZATION School of Engineering	6b. OFFICE SYMBOL <i>(If applicable)</i> AFIT/ENG	7a. NAME OF MONITORING ORGANIZATION		
6c. ADDRESS (City, State, and ZIP Code) Air Force Institute of Technology Wright-Patterson AFB, OH 45433-6583		7b. ADDRESS (City, State, and ZIP Code)		
8a. NAME OF FUNDING / SPONSORING ORGANIZATION AFEWC	8b. OFFICE SYMBOL <i>(If applicable)</i> SAX	9. PROCUREMENT INSTRUMENT IDENTIFICATION NUMBER		
8c. ADDRESS (City, State, and ZIP Code) Air Force Electronic Warfare Center San Antonio, TX 78243-5000		10. SOURCE OF FUNDING NUMBERS		
		PROGRAM ELEMENT NO.	PROJECT NO.	TASK NO.
		WORK UNIT ACCESSION NO.		
11. TITLE (Include Security Classification) MODELING THE IMPULSIVE RESPONSE OF A MONOPULSE RADAR TO IMPULSIVE JAMMING SIGNALS USING THE BLOCK ORIENTED SYSTEM SIMULATOR (BOSS)				
12. PERSONAL AUTHOR(S) Jeffrey K. Long, Capt USAF				
13a. TYPE OF REPORT MS-Thesis	13b. TIME COVERED FROM _____ TO _____	14. DATE OF REPORT (Year, Month, Day) 1989 December	15. PAGE COUNT 88	
16. SUPPLEMENTARY NOTATION				
17. COSATI CODES			18. SUBJECT TERMS (Continue on reverse if necessary and identify by block number) Radar Jamming, radar countermeasures, Monopulse Radar	
FIELD	GROUP	SUB-GROUP		
17	04	03		
17	09			
19. ABSTRACT (Continue on reverse if necessary and identify by block number) Thesis Chairman: Lt Col David Meer				
20. DISTRIBUTION / AVAILABILITY OF ABSTRACT <input checked="" type="checkbox"/> UNCLASSIFIED/UNLIMITED <input type="checkbox"/> SAME AS RPT <input type="checkbox"/> DTIC USERS		21. ABSTRACT SECURITY CLASSIFICATION UNCLASSIFIED		
22a. NAME OF RESPONSIBLE INDIVIDUAL Lt Col David Meer		22b. TELEPHONE (Include Area Code) (513) 255-3576	22c. OFFICE SYMBOL AFIT/ENG	

19. cont.
ABSTRACT:

The purpose of this study was to develop computer models of two types of amplitude comparison monopulse processors using the Block Oriented System Simulation (BOSS) software package and to determine the response to these models to impulsive input signals. This study was sponsored by the Air Force Electronic Warfare Center at Kelly AFB in an effort to determine the susceptibility of monopulse tracking radars to impulsing jamming signals.

Two types of amplitude comparison monopulse receivers were modeled, one using logarithmic amplifiers and the other using automatic gain control for signal normalization. Simulations of both types of systems were run under various conditions of gain or frequency imbalance between the two receiver channels. The resulting errors from the imbalanced simulations were compared to the outputs of similar, baseline simulations which had no electrical imbalances.

The results of the analyses showed that the accuracy of both types of processors was directly affected by gain or frequency imbalances in their receiver channels. In most cases, it was possible to generate both positive and negative angular errors, dependent upon the type and degree of mismatch between the channels. The system most susceptible to induced errors was a frequency imbalanced processor which used AGC circuitry. This research also demonstrated that any errors introduced will be a function of the degree of mismatch between the channels and therefore would be difficult to exploit reliably. It is recommended that further research be conducted with both amplitude and phase comparison monopulse processors to further quantify the nature of the errors that can be introduced into these systems with an impulsive jamming signal.